DETECTION OF LONGITUDINAL TOOTH FRACTURES USING LOCAL COMPUTED TOMOGRAPHY

By

Maria Alejandra Mora

A thesis submitted to the faculty of the University of North Carolina at Chapel Hill in partial fulfillment of the requirements for the degree of Master of Science in the Department of Diagnostic Sciences and General Dentistry, School of Dentistry**.**

Chapel Hill

2006

Approved by:

Advisor: Dr. André Mol. DDS, MS, PhD

Reader: Dr. Donald A. Tyndall. DDS, MSPH, PhD

Reader: Dr. Eric M. Rivera. DDS, MS

ABSTRACT

MARIA ALEJANDRA MORA

"Detection of Longitudinal Fractures Using Local Computed Tomography (LCT)" (Part I), and "Effect of the Number of Basis Images in the Detection of Longitudinal Fractures Using Local Computed Tomography (LCT)" (Part II)

(Under the direction of Dr André Mol)

The purpose of this study was to test the feasibility of Local Computed Tomography (LCT) for the detection of longitudinal fractures and to determine the effect of the number of basis images on the detection accuracy.

In Part I, 10 observers' evaluated LCT image volumes generated with 180 basis images of fractured and non-fractured teeth. These were compared with conventional radiographs to assess the accuracy in detecting longitudinal fractures.

Part II evaluated the effect of the number of basis images on the detection of longitudinal fractures. 180, 60, 36 and 20 basis images were tested.

This study demonstrated that LCT provided a significant improvement in the accuracy of detecting longitudinal fractures compared to periapical radiographs. LCT maintains its efficacy for detecting longitudinal fractures with 60 instead of 180 basis images. A subsequent reduction to 36 basis images significantly reduced the detection rate.

“The hardest arithmetic to master is that which enables us to count our blessings”

Eric Hoffer

A mis padres por el amor dado y por ser la luz que ha iluminado mi camino todos estos anos. A mis amados hermanos por caminar conmigo de la mano en este viaje.

To my parents for all their love and for being the light that has guided me through the path throughout the years and to my beloved siblings, for walking hand to hand with me in this journey.

TABLE OF CONTENTS

LIST OF TABLES

Page

LIST OF FIGURES

Page

LIST OF ABBREVIATIONS

2D	Two dimensional
3D	Three dimensional
ANOVA	Analysis of Variance
Az	Area under Receiver Operating Curve
.buf	Raw image file format extension
CBCT	Cone Beam Computed Tomography
CCD	Charged Couple Device
CEJ	Cemento Enamel Junction
CMOS	Complementary Metal Oxide Semi-Conductor
Cm	Centimeter
CT	Computed Tomography
DF	Degrees of Freedom
DICOM	Digital Imaging & Communications in Medicine
FPD	Flat Panel Detector
.gipl	Guy's Image Processing Library image file format
Kvp	Kilovolt Peak
LCT	Local Computed Tomography
mA	Milliamperage
mm	Millimeter
MPR	Multiplanar Reconstruction/ reformatting
OSD	Object-to-Sensor Distance
PDL	Periodontal Ligament
.raw	Raw image file format extension

ROC	Receiver Operating Characteristics
ROI	Region of Interest
SD	Standard Deviation
SNR	Signal-to-Noise Ratio
SOD	Source-to-Object Distance
TACT	Tuned Aperture Computed Tomography
VRF	Vertical Root Fracture

INTRODUCTION

Background and Significance

Longitudinal fractures are characterized by an incomplete or complete fracture line that extends through the long axis of the tooth.[1-4]. These fractures occur primarily in the vertical plane, i.e. in the direction of the long axis of the crown or the root.[3] Although they can occur in all teeth, they are more prevalent in posterior teeth. Longitudinal fractures are caused by excessive forces from mastication or occlusion, either large forces on a normal tooth or normal forces on a weakened tooth.[4] Root fractures may originate at the coronal level or at the apex. [5-7] The term *longitudinal* describes the linearity of these fractures and the fact that they grow and change over time.[3] Some are not difficult to manage, whereas others represent irreversible damage to the tooth requiring extraction.[3]

Walton and Rivera have classified longitudinal fractures into five distinct groups, generally from least to most severe: (1) craze lines, (2) fractured cusp; (3) cracked tooth; 4) split tooth; and (5) vertical root fractures.[8,3] Longitudinal fractures have been confused or combined in clinical articles, resulting in misunderstanding and incorrect diagnoses and treatment.[2, 8] Cracked tooth, split tooth and vertical root fracture involve the root and are able to compromise the periodontium.

Cracked teeth are incomplete fractures that usually involve mandibular molars (restored and non-restored) followed by maxillary premolars and maxillary first molars.[4, 9, 10] Cracks in teeth are almost invariably mesiodistal fractures, although mandibular molars occasionally fracture toward the facial-lingual surface. Fractures originate on the occlusal surface and grow towards the cervix and down the root. Importantly, the more centered the fracture (originating in the middle of the occlusal surface), the more likely it will extend deeper before it shears towards the root surface.[4] Cracks can cross one or both marginal ridges. They generally shear towards the facial and lingual side toward a root surface, usually lingual.[4] Cracked teeth are predominantly seen in older patients, although they may occur at any age in adults.[9, 11] The longevity and complexity of restorations also seem related, although cracked teeth are commonly minimally restored.[10 12] More years of mastication, particularly of hard objects, also plays a role. Continued and repeated forces fatigue tooth structure and can result in a small fracture followed by its continued growth.[10] The prognosis for this type of fracture depends on the severity of the crack. A cracked tooth that is not treated will progressively worsen. It can evolve into a split tooth or result in severe periodontal defects.[4] Eventually, the tooth may be lost. Therefore early diagnosis and treatment are essential in saving these teeth.

A split tooth is often the result of the long term progression of a cracked tooth where there are two distinct segments that can be separated from one another. These teeth are associated with the same factors related to cracked teeth. They may be more frequent in root canal treated teeth and in teeth that have been compromised by caries, restorations or an over-extended access preparation.[11]

These fractures extend primarily in a mesio-distal direction crossing both marginal ridges and extending deep into the root to shear the root surface in the middle or apical third. The more the fracture is centered on the occlusal surface, the greater the tendency to extend apically. [4] The extent and position of the crack will determine whether any portion can be maintained. However, most of these teeth will be extracted. Unfortunately, even though there has been an advance in the way teeth are treated, a split tooth can never be saved intact.

Vertical root fractures (VRF) are defined as longitudinal fractures confined to the root that usually begin on the internal canal wall and extend outward to the root surface. They occur primarily in the facial-lingual plane. Certain root shapes and sizes are more susceptible to VRF. Roots that are deep facially and lingual but narrow mesially and distally are particularly prone to fracture.[13] Examples are mandibular incisors and premolars, maxillary second premolars, mesiobuccal roots of maxillary molars and distal roots of mandibular roots. [4]The fracture probably begins internally and grows outwards to the root surface.[4] The fracture may begin at the apex or mid-root,[5] therefore, it may be incomplete extending neither to the facial and lingual root surfaces nor from the apical to the cervical root surface.[4] The cause of these fractures is mainly iatrogenic, i.e. extensive dental treatment. Examples are excessive canal shaping, excessive pressure during compaction of gutta-percha, excessive width and length of a post space in relation to the tooth's anatomy and morphology, or excessive pressure during the placement of a dowel.[2] VRF in non-endodontically treated teeth that are not a continuation or apical extension of a cracked or split tooth are not uncommon according to a study done in a Chinese population.[14] Vertical root fractures often present no specific signs and symptoms and therefore it is difficult for dentists to make a definite diagnosis of the condition.[14] Because treatment is invariably tooth extraction or removal of the fractured root, diagnosis is critical.[3] Prognosis is virtually hopeless for teeth with a vertically fractured root.[4]

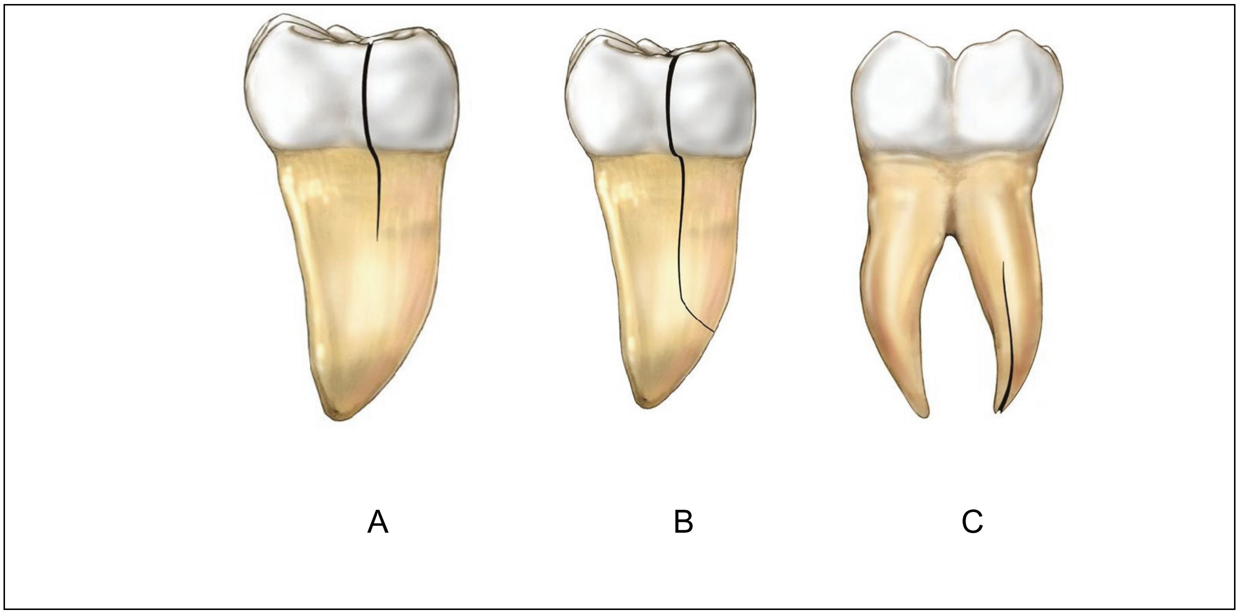

Fig 1. Longitudinal Fractures. (A) Cracked tooth, (B) Split tooth, and (C) Vertical root fracture.

The incidence of longitudinal fractures is apparently increasing. One reason is the increasing age of patients with decreasing number of tooth extractions. More teeth undergo complex procedures and are present for longer periods of time. Restorative and endodontic treatments remove dentin, thus compromising the internal strength of the tooth. In addition, teeth absorb external forces, usually occlusal, that exceed the strength of dentin and gradually alter the tooth structure. When the destructive force is beyond the elastic limit of dentin or enamel, a fracture occurs. Therefore, the longer a tooth is present and the more forces it undergoes, the greater the chances of an eventual fracture. The second reason for the increase in incidence is that there is more awareness and better diagnosis and identification of the problem. These fractures are not confined to elderly patients and do not occur only in restored teeth.[8]

The occurrence of both cracked teeth and split teeth is unknown but it is apparently increasing.[12, 15, 16] Many factors related to cracked teeth are endemic to split teeth.[4] The overall occurrence of VRF is unknown, but they are common. Fuss and coworkers found a prevalence of 10.9% for VRF's.[17] This number was close to that found by Vire of 12.9%.[18] The high prevalence of Vertical Root Fractures can be explained by the fact that the final diagnosis of VRF was obtained after the tooth was extracted and the fracture could be demonstrated visually. Previously reported clinical and radiographic retrospective surveys found lower percentages: 4% (Hansen and coworkers)[19], 3.7% (Morfis)[20], and 2.6% (Torbjorner and coworkers).[21] Most likely, the lower incidence levels are related to the difficulties in the clinical diagnosis of vertical root fractures. Sjogren and coworkers[22] evaluated 635 endodontically treated teeth in a success and failure study for a period of 8-10 years and found a prevalence of 30.8% being the highest percentage ever reported in an extracted tooth population.[17]

There is relatively little research on longitudinal tooth fractures, particularly on clinical outcomes related to diagnosis and treatment.[23] The literature suggests that conventional diagnostic methods to detect dentoalveolar fractures exhibit low diagnostic efficacy.[17, 21] This is evident from the large variations in prevalence rates reported in some studies.[24]

Diagnosis of these different entities is necessary in order to select a treatment that suits the conditions of the tooth when a fracture is present. Dental history, clinical assessment of the tooth accompanied by diagnostic tests such as transillumination, flap reflection, tooth slooth instruments, dyes and radiographs serve as aids in the detection of these fractures. One of the biggest challenges for endodontists is the fact that they are working in areas that cannot be visualized clinically. It is for this reason that conventional radiography continues to be the most commonly used imaging modality for diagnosing fractures of the root in endodontically treated teeth.[25] Preoperative radiographs aid in visualizing the anatomy of the root canal system, the periodontium and identifying the presence of pathoses.

Cracked teeth are difficult to be seen radiographically due to the direction of the fractures. Conventional radiography serves as an aid in assessing pulpal and periodontal compromise but give little or no information on the direction and extent of the fracture. Depending on the extension towards the root and the relationship with the periodontium (below alveolar crest) the treatment is going to vary. If the fracture is contained to the crown surface it can be restored. If a fracture extends below the alveolar crest, the prognosis is worse. Making the proper treatment decision is a challenge for the endodontist as there are limited non-invasive tools to assess the length of the fractures below the soft tissues and alveolar crest.

Split teeth do not have the same variety of confusing signs, symptoms, and test results as cracked teeth.[4] Generally, split teeth are easier to identify.[16] Findings on radiographs depend partially on pulp status, but are more likely to reflect damage to the periodontium. Often there is marked horizontal loss of interproximal or interradicular bone.[16] Radiographs show the same signs as with cracked teeth, i.e. signs of compromised adjacent structures. When the fragments of tooth are displaced, the fracture can usually be detected radiographically.

Radiographic features of vertical root fractures may imitate periodontal disease or root canal treatment failure.[26] Only in a small percentage of teeth a visible separation of fractured root segments can be seen.[4] Deep periodontal pockets result from chronic localized inflammation as time progresses. It has been shown that the radiolucencies and the signs and symptoms can manifest themselves days, weeks, or even years after the fracture.[27] Delay in the appearance of the pockets can be explained by the fact that when VRF is not yet complete, the fracture does not extend from one side of the root to the other. Most of the coronal margin of the fracture is situated apically to the epithelial attachment and, as a result, the pocket will not form.[27] It has also been reported by Meister and coworkers that periapical or periodontal radiolucencies do not appear in all VRF cases.[28] False positive diagnoses can also result from detection of radiographic signs indicative of superimposed normal anatomy such as the periodontal ligament space of a buccal/lingual root in multi-rooted teeth. This is undesirable since teeth may unnecessarily be extracted in these cases.[24]

In general, for relatively non-displaced fractures, superimposition of overlying and adjacent anatomical structures and a beam direction that is not parallel to the fracture line impede the radiographic detection of vertical root fractures.[24] These longitudinal fractures are commonly challenging and in many cases present problems with diagnosis and treatment.[3,29] Radiographs are helpful but are not solely diagnostic except in those few instances in which the fracture is obvious.[4] These fractures may be difficult or impossible to visualize and not demonstrable until they grow larger.[3] Moreover, superimposition of structures can be a major difficulty in fracture detection and identification of associated pathologic processes. Clinical diagnosis of this type of fractures is difficult as the symptoms are nonspecific and may resemble endodontic treatment failure or periodontal disease.[30]

The limitations of conventional radiography are related to the lack of depth-specific information.[24] Structures with a three-dimensional nature, like longitudinal fractures, are particularly difficult to assess. The reason for this is that conventional radiography provides 2D images of 3D structures. Although intraoral imaging has a number of inherent limitations, low dose, low cost and ease of operation has made it the preferred tool for the assessment of hard tissues, both for the evaluation of treatment outcomes and as a baseline for future assessment.

The introduction of digital imaging in dentistry generated many new research initiatives aimed at unlocking the diagnostic potential of radiography through image processing. Some of these initiatives have resulted in meaningful applications that have been shown to increase the diagnostic utility. While these applications are not yet easily implemented in a clinical setting, they begin to address some of the diagnostic imaging needs in endodontics in terms of early detection and localization assessment.

Many studies have tried to find alternatives to correctly diagnose longitudinal fractures. Examples of these are studies that have compared two intraoral digital systems with the results showing no significant differences in the diagnostic accuracy.[31] Studies on the effect of altered image size on the diagnostic assessment of root fractures found no improvement in the detection either.[32]

The inability of conventional imaging modalities to adequately visualize vertical root fractures indicates the need for the development and study of alternative diagnostic imaging systems that carry the potential of improving the detection of vertical root fractures.[24]

Advances in basic endodontic research have transformed our understanding of almost all aspects of the endodontic disease process. These developments have translated into meaningful clinical applications improving the way we diagnose and treat diseased teeth. In comparison, the impact of radiographic imaging on the management of the endodontic patient has essentially remained unchanged for decades. Substantial advances in x-ray generator and x-ray detector technology have resulted in significant dose reductions and improved image quality. However, with the exception of digital subtraction radiography, the basic information content of oral radiographic images has changed very little.

Problem definition

At present, it remains virtually impossible for endodontists to gather complete and accurate 3D information in order to detect non-displaced root fractures in a clinical setting. Current imaging modalities provide incomplete data and measurements are susceptible to various sources of error. These limitations weaken the diagnostic process, both in the initial work-up and during follow-up. The time between completion of treatment and VRF diagnosis is an important factor, because future restoration will also depend on the amount of remaining bone after extraction.[33] In addition, the poor prognosis of the condition coupled with clinical and financial consequences for the patient demands improvement in the diagnostic tools used currently for early detection of these fractures. [34]

In order to overcome the radiographic detection problem, an imaging system is needed that will provide images with high spatial resolution in order to detect narrow non-displaced fractures and 3D visualization of the teeth. Although the technology to generate 3D radiographic images is available, most 3D imaging technologies require highly specialized equipment, are costly and dose intense. The current armamentarium for acquiring dental radiographic images has been considered inadequate for generating 3D images. Advances in image processing have made it possible, however, to synthesize meaningful 3D reconstructions with relatively simple equipment. Multiple views of an area of interest can be used to synthesize new images that can aid the clinician in making accurate diagnoses. The added benefit of the information needs to outweigh the extra costs associated with the increased sampling rate, both economically and in terms of absorbed dose. Thus, the broad research question is: can we develop an imaging technique that allows the clinician to visualize longitudinal fractures in 3D with a favorable cost-benefit ratio?

Review of potential solutions

Three-dimensional information can only be obtained when multiple views are obtained. In its simplest form, two images taken with a small angular disparity can be used to generate a stereoscopic view. When more than two images with different projection angles are combined, views can be synthesized that provide some 3D information. As the disparity of projection angles increases, a more complete 3D model can be generated. The maximum disparity of 360 degrees is used by computed tomography allowing a complete 3D image representation of the tissues. The following sections briefly review current methods for acquiring 3D image data in dentistry.

Tuned Aperture Computed Tomography (TACT™)

TACT was developed to achieve 3D imaging with existing dental equipment and without the high cost and dose associated with computed tomography. TACT is built on the basic principles of tomosynthesis: by shifting and combining a set of basis projections, arbitrary slices through the object can be brought into focus.[35-37] Results of studies testing TACT for the detection of artificially induced vertical radicular fractures have indicated that the diagnostic accuracy is higher than that of conventional radiographs.[24] Most studies have used relatively small angular disparities between basis projections. This puts an upper limit on the amount of 3D information that can be gathered. At this point it remains uncertain whether TACT will ultimately be used in the dental clinic.

Computed Tomography (CT)

CT generates a sliced image volume that can be visualized in various orientations through a process called multi-planar reformatting (MPR). Most software applications are also capable of rendering 3D surfaces and volumes, allowing the clinician to study the various tissues in a more intuitive manner. While CT provides exquisite three-dimensional views, its ability to show very small details remains limited, usually not more than 1-2 millimeter. Currently, thin multi-slice spiral CT is capable of rendering uniform sub-millimeter resolution in all three dimensions (isotropic pixels). Although the level of image detail remains considerably lower than with conventional intraoral imaging, the advancements in CT technology satisfy important endodontic imaging needs. Youssefzadeh and coworkers studied the value of CT in the diagnosis of vertical root fractures relative to the value of conventional radiography and found that CT is superior to dental radiography in the detection of displaced fractures.[32] The drawback of this study was the type of fractures studied. Non-displaced fractures and incomplete fractures make the diagnostic task more challenging. In addition, the application of CT imaging for endodontic diagnosis has an unfavorable cost-benefit ratio. Studies have shown that the effective dose of CT for imaging the mandible and the maxilla is much higher than with conventional radiography.[38, 39] While developments in CT scanner technology continue to reduce patient dose, the acquisition of high-resolution CT images remains a high-dose procedure. Other drawbacks include the limited availability of medical CT imaging to dental health care providers and the cost of obtaining and reformatting a scan for this purpose, which is often prohibitive.[39]

Cone-beam CT (CBCT)

A new generation of compact CT scanners has been developed specifically designed for imaging the head and neck region.[40] CBCT uses a cone-beam x-ray geometry with an area detector rather than a fan-beam geometry with a linear detector. The cone-beam geometry improves data acquisition efficiency and x-ray photon utilization. Spatial resolution and spatial resolution uniformity are generally higher, which has facilitated significant advancements in clinical three-dimensional CT applications.[41] CBCT units impart a much lower dose to the patient and their simplified design significantly lowers their cost.[42] The main drawback of the cone-beam geometry is the increase production and detection of scatter radiation. This limits CBCT scanners in imaging subtle tissue contrast as exists between various soft tissues. Their main application is therefore in hard tissue imaging.

Currently, there are two approaches in selecting the area detector. One uses an image intensifier; the other uses a flat panel detector (FPD). While FPDs are the large area detectors of the future, their high cost (and higher dose requirement) has made image intensifiers the detector of choice for most companies bringing CBCT units to the market. These include the NewTom QR-DVT-9000 (QR-NIM s.r.l., Verona, Italy), [43] Hitachi CB MercuRay (Hitachi Medico Technology Co., Ltd, Chiba, Japan), [44] and other prototype units.[45] At present, only the i-CAT unit (Imaging

Sciences International, Hatfield, PA) has been developed with a FPD.[40] CBCT scanners will become a major asset in oral and maxillofacial imaging, making CT available for a broader range of diagnostic problems in dentistry. Moreover, the CBCT modality will be a powerful platform for developing novel diagnostic imaging applications. In order to achieve the high resolution requirements of some dental diagnostic procedures, such as imaging of dental fractures and radicular structures, a specialized form of CBCT, called Local CT, is currently under development.

Local CT (LCT)

Local CT also uses a cone-beam x-ray geometry, but the beam diameter is smaller than the volume being scanned. While this reduces the dose to the patient, it implies that the sampling is complete only in the region of interest (ROI) covered by the x-ray beam in each of the basis projections.[46] Initial studies have shown the feasibility of LCT *in vitro* and its ability to improve the detection of proximal caries.

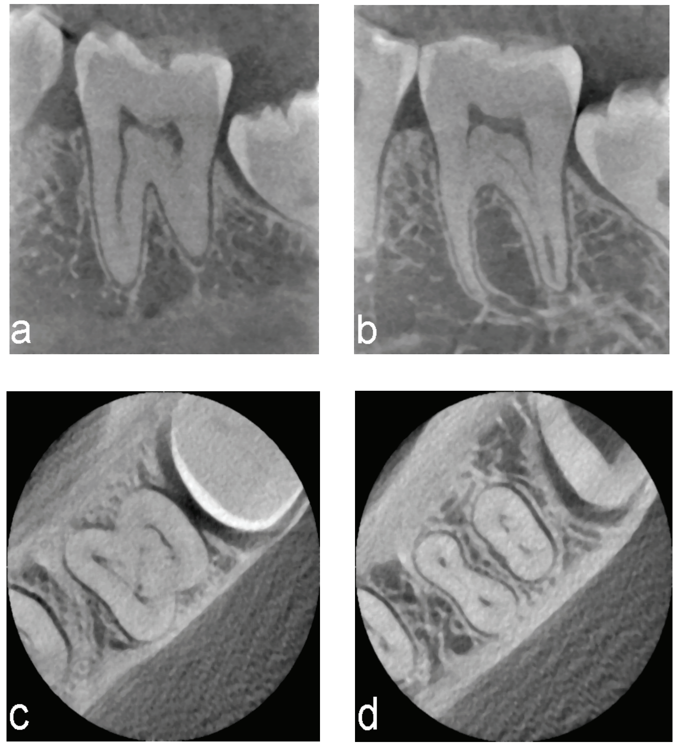

Fig 2. Examples of image slices created with Local CT using and intraoral sensor. Two sagittal cross-sections (a and b) and two axial cross-sections (c and d). Courtesy A.N. van Daatselaar et al., Amsterdam, The Netherlands.

The basic setup consists of a standard intraoral x-ray unit with a small focal spot. A long source-to- object distance (SOD) and a collimator between the x-ray unit and the object are used in order to approximate the cone beam with a parallel beam. When parallel rays are assumed, only 180 basis images are necessary to create the volume. Additional basis images would result in duplication of data. For ease of experimentation in the *in vitro* stage, an object has to be placed on an automated rotating table. Basis projections at different angles are acquired with a standard intraoral solid-state detector based on either charge-coupled device (CCD) or complementary metal oxide semi-conductor (CMOS) technology. Generally, the detectors have a pixel sizes in the order of 20-50 μm and an active area similar to that of a size-2 film (approximately 30 x 40 mm). With these types of detectors, CT images of dentoalveolar tissues can be generated with very high resolution. A reconstruction algorithm (filtered back projection) similar to the one used for CT is used in this type of setup. Slices are calculated from the basis images taken from different angles. The information about the slice is contained in a single row of pixels in each of the images of the series of projections. The information in other slices is represented in the corresponding other rows of the projections. The rows for a particular slice can be collected in a new image called a sinogram. The height of the sinogram corresponds to the number of slices and the width is the same as the width of the projections. The filtered backprojection (algorithm) takes each row of the sinogram and projects it in the direction in which the projection was made. The backprojections adds all of the projections creating the image volume. Filters are used to modify the profiles of the resultant histograms. The use of filters creates images with better quality and with better visual contrast.[47] In Van Daatselaar's work, the reconstruction algorithm used the combination of a ramp filter and a Hamming filter. The Hamming filter was chosen because it provided better contrast between background and object. This is an important factor since adjacent tissues contribute to a decrease in contrast in the region of interest (ROI). The back-projection algorithm produces a blurry version of the desired image. In the absence of noise, the desired image can be obtained by filtering the back-projection with a ramp filter. The problem with this is the high-pass nature of the ramp filter which leads to amplification of high-frequency noise. For this, it is best to use a low pass filter to reduce the noise. The reformatted images of dental hard tissues result in images that exhibit good contrast and spatial resolution with a high signal-to-noise ratio (SNR) (Figure 2).

The characteristics of LCT are conducive to extracting reliable 3D quantitative data. Current research efforts are aimed at investigating optimal scanning schemes, balancing the need for high image quality and a low number of basis projections in order to lower the dose. The initial research done by Van Daatselaar used a set of 100 basis projections, but later data suggested that basis projections as few as 14-20 yield diagnostically useful images. The problem with the reduction of basis images is that image quality is compromised due to the fact that less information of a volume is gathered. Image quality reduction includes: low signal-to-noise ratio, enhancement of artifacts and low contrast resolution.

Recently, the Morita 3D Accuitomo (J. Morita Co., Tokyo, Japan) was introduced. This CT unit was specifically designed for oral and maxillofacial imaging using a limited field of view. This system achieves a higher resolution than other CBCT systems, although its resolution remains somewhat limited by the use of an image intensifier.[48-51] There are currently no data regarding the accuracy of LCT images for extracting quantitative data, either manually or automatically. Accordingly, there is no information on the relationship between acquisition parameters and the ability to obtain meaningful data for clinically relevant tasks.

The Vision

The vision that motivated this research was to develop a radiographic imaging modality that allowed high-resolution visualization of longitudinal fractures. The ultimate goal was to develop an imaging system that provides high quality 3D images of the dento-alveolar tissues and that does not rely on placing image receptors in the patient's mouth. The goal of the current study was to provide feasibility data and to demonstrate that a clinically meaningful diagnostic problem can be solved, i.e. gathering 3D data of the roots of fractured teeth. Specifically, the purpose of this study was to test the hypothesis that Local Computed Tomography (LCT) would allow reliable detection of longitudinal fractures. This also includes the investigation of the effect of number of basis images on detection accuracy of these fractures.

MANUSCRIPT I

DETECTION OF LONGITUDINAL TOOTH FRACTURES USING LOCAL COMPUTED TOMOGRAPHY

Abstract

Objective: To test the accuracy of Local Computed Tomography (LCT) in detecting longitudinal fractures in comparison with conventional periapical radiographs.

Study Design: Longitudinal fractures were induced in 30 of 60 teeth. The teeth were placed in a dry dentate mandible with soft tissue simulation. A laboratory LCT unit was used to acquire 180 basis projections with 1^{o} separation along an 180^{o} arc. Conventional radiographs served as the control modality. Correlated axial, coronal and sagittal views were presented to 10 observers. The observers determined the presence of a root fracture using a 5-point ROC confidence scale.

Results: The mean A_z for LCT was 0.91 (SD=0.07). The mean A_z for conventional radiography was 0.70 (SD=0.07). The difference between the modalities was statistically significant (ANOVA: $p<0.0002$), whereas the differences between the observers was not (ANOVA: $p=0.319$).

Conclusion: Local CT significantly improves the detection of longitudinal fractures *in vitro* compared to conventional periapical radiography.

INTRODUCTION

Longitudinal tooth fractures are characterized by an incomplete or complete fracture line that extends through the long axis of the tooth.[1] The term longitudinal describes the linearity of these fractures and the fact that they grow and change over time.[2] They have been classified into five distinct groups, generally from least to most severe: (1) craze lines, (2) fractured cusp; (3) cracked tooth; 4) split tooth; and (5) vertical root fractures.[3] Although these types of fractures can occur in all teeth, they are more prevalent in posterior teeth. They may be caused by excessive forces from mastication or occlusion, either large forces on a normal tooth or normal forces on a weakened tooth.[4] Longitudinal fractures may originate at the coronal level or at the apex.[5-7] The prognosis of a tooth with an extensive fracture is poor and in many cases extraction is the only possible treatment option.

The incidence of longitudinal fractures is unknown, but is thought to be increasing as a result of greater longevity of patients. Also, teeth are in the mouth longer and are more likely to undergo complex procedures. Restorative and endodontic treatments that remove dentin compromise the internal strength of the tooth.[3]

The detection of non-displaced longitudinal fractures, such as cracks and vertical root fractures, is a significant challenge in clinical practice. Clinical diagnosis of longitudinal fractures is difficult as the symptoms are variable or nonspecific and may even resemble post-treatment disease following root canal treatment or periodontal disease.[8] Radiographic signs are usually absent when the orientation of the x-ray beam is not parallel to the plane of the fracture.[9] Superimposition of other structures further limits the sensitivity of radiographs for the detection of longitudinal fractures. The two-dimensional nature of conventional radiographs limits its ability to reveal longitudinal fractures. It appears that a high-resolution image modality providing a three-dimensional view of the root can improve the detection rate. Local Computed Tomography (LCT) represents such a modality. It uses a cone-beam x-ray geometry with a small field of view and a high-resolution detector. The feasibility of LCT has been demonstrated previously.[10, 11]

The purpose of this study was to test the accuracy of Local Computed Tomography (LCT) in detecting longitudinal tooth fractures in comparison with conventional periapical radiographs.

Materials and Methods

An *in vitro* model was used consisting of 60 extracted human teeth (Table1). Longitudinal fractures were induced in 30 of these teeth. For all teeth, endodontic access openings were made and the canals were located. The roots of the teeth selected to be fractured were placed in acrylic in order to prevent splitting of the roots. A thin layer of wax was applied to allow the teeth to be removed. A screwdriver type wedge was placed in the canals and fractures were induced using controlled pressure applied by gentle tapping. As a result, the fractures originated from within the root. In order to prevent the induction of a displaced fracture, the progression of the fracture was monitored by removing the tooth from the acrylic.[12] A set of 30 matching teeth without fractures were selected to serve as controls. The entire sample was kept hydrated during the entire process except during fracture induction and radiographic scanning. Prior to scanning, each tooth was placed in a dentate dry mandible and was held in place in the alveolus with boxing wax and orthosil (Orthosil Silicone Dental “Wax”, DentaKit ^{TM}, Belmont, CA). Orthosil served as a surrogate for trabecular bone. A mixture of natural grains was mixed in the orthosil to simulate marrow spaces. The dry mandible was covered with boxing wax to simulate soft tissues.

Image acquisition

The basic components of the *in vitro* LCT imaging system included a conventional cone-beam dental x-ray source (Planmeca Prostyle Intra, Planmeca OY, Helsinki, Finland), an object stage and a high-resolution digital x-ray detector. The components were mounted on an optical rail with micro-positioning equipment (Spectra-Physics, Mountain View, CA). For ease of experimentation, the mandible rotated while the source and the detector were stationary. The x-ray generator was fixed on a translator to allow adjustment of the central ray. The mandible was placed on a motorized rotator which, in turn, was mounted on high-precision translators. This allowed accurate positioning and computer-controlled rotation of the mandible relative to the x-ray beam and the x-ray detector. A size-2 Schick CDR DICOM sensor served as the x-ray detector (Schick Technologies, Inc., Long Island City, NY). This detector is capable of producing images with a linear gray scale of 12 bits per pixel, i.e. 4096 gray levels. The pixel size is 40μm x 40μm. The sensor was mounted on a precision rotator to align the detector matrix with the object rotation axis. Exposure settings were set at 70 kVp, 8 mA and 1.25 seconds. The source-to-object distance and object-to-sensor distance were fixed at 65 cm and 12.5 cm, respectively. Image acquisition was controlled by three synchronized software programs for image capture, rotation of the stage and exposure. Prior to scanning the sample, calibration was performed in order to align the central ray, the center of rotation and the center of the sensor. The mandible was mounted on the rotating stage with the tooth of interest placed in the center of rotation. 180 basis images were taken with one degree separation along an 180^{o} arc. The basis images were exported from the Schick CDR software and converted to raw images. The image volume was generated from the raw images using a filtered back projection reconstruction algorithm.[10] Five slices were averaged, thus generating axial slices with a thickness of 0.2 mm (5x40μm). The axial slices were opened in ImageJ (Version1.34s. Wayne Rasband, National Institutes of Health, USA) and saved as a stack of raw images. Axial slices showing the crown were eliminated in order to prevent the status of the crown to bias an observer's assessment of the root. The reduced stack of images was then converted to GIPL (Guys Image Processing Lab) format. The GIPL conversion was required in order to view the image volume using the IRIS 2000 software (Department of Computer Sciences, The University of North Carolina at Chapel Hill, Chapel Hill, NC). IRIS 2000 provides multi-planar reconstruction of an image volume and displays three windows of correlated axial, coronal and sagittal planes (Figure 3).

Conventional intraoral radiographs were acquired immediately after each LCT scan using a Kodak RVG 6000 sensor (Eastman Kodak, Rochester, NY). The crowns of the teeth were masked with an opaque overlay up to the cemento-enamel junction (Figure 4).

Observation sessions

Ten observers were recruited for the study. The group consisted of four radiologists, one radiology resident, four endodontic residents, and one periodontist. Prior to the actual assessment, the observers were trained on three separate sets of LCT images that were not part of the sample. Images were coded and randomized. Half the observers first viewed LCT images, the other half first viewed conventional images. All images were displayed on a 21.3 inch true color flat panel monitor (Samsung, Sync Master 213T, Samsung Electronics co., ltd, Ridgefield Park, NJ) at its native resolution of 1600x1200 pixels under dimmed ambient lighting.

Conventional images were presented as a stack using ImageJ against a black background. LCT images were presented in IRIS 2000. The observer was able to align the three planes at any point by clicking a location of interest in any one of the planes (Figure 3). The observers were encouraged to browse through the images and modify brightness and contrast. They were asked to assess the presence or absence of a longitudinal fracture. They recorded their response on a 5-point probability scale as follows: 1=fracture definitely not present; 2=fracture probably not present; 3=unsure; 4=fracture probably present; 5=fracture definitely present. Receiver operating Characteristic (ROC) curves were constructed for each observer and each modality using the ROCKIT software (Version 0.9, Charles E Metz, The University of Chicago, Chicago, IL).

Ground truth

The entire sample was removed from the hydrated environment, air dried and stained using 1% methylene blue. The dye was placed in the canal and allowed to flow through the fracture if present. The presence of fractures was assessed visually by a single person. The absence of fractures in the control teeth was also confirmed through this process.

Statistical analysis

Differences between the areas under the ROC curves (A_z) were analyzed with ANOVA to test the null–hypothesis of no difference between the two imaging modalities and the observers.

Results

Table 2 shows the areas under the ROC curves (A_z) for each observer and modality. Observer #6 did not use the entire range of the ROC scale, which resulted in degenerative data for ROC analysis. LCT resulted in a mean A_z of 0.91 (SD=0.07) and conventional radiography in a mean A_z of 0.70 (SD=0.07). Figure 5 shows the ROC curves for both modalities based on pooled data from all observers. Analysis of variance (Table 2) showed that there was a statistically significant between the modalities ($p< 0.0002$), but no statistically significant difference between observers ($p= 0.319$).

Discussion

The introduction of 3D cone-beam CT has dramatically changed the diagnostic capabilities in dentistry. 3D images can be generated at relatively low doses and with high resolution compared to conventional CT. Recognizing the high resolution requirements for oral and maxillofacial applications, a cone-beam CT system was developed with a smaller field of view.[13-15] Van Daatselaar and coworkers took this concept one step further by using a high-resolution intraoral sensor as the image detector. Their studies demonstrated the feasibility of Local CT (LCT) and its ability to improve caries detection relative to conventional radiography.[10, 11] While still in its infancy and with many problems remaining to be solved, demonstrating the feasibility of LCT for solving other diagnostic problems has become a driving force behind its further development. The detection of longitudinal fractures represented a suitable and clinically relevant diagnostic problem in this regard.

This study demonstrated that LCT provided a significant improvement in the accuracy of detecting longitudinal fractures compared to periapical radiographs. While the comparison to conventional radiography appears unfair, the use of conventional radiographs in this study served to demonstrate that detection of the fractures represented a true challenge to the observers. It was noted that for most observers, the A_z values for conventional radiography were not as low as expected, with a positive outlier as high as 0.82. This implies that longitudinal fractures actually do result in detectable radiographic signs or that the *in vitro* model was not an ideal simulation of the actual clinical world. Limitations of the model included the method of fracture induction and the environment in which the teeth were placed. The fact that there was no real bone surrounding the tooth and the lack of periodontal ligament (PDL) may have played a role in enhancing fracture visibility in conventional radiographs. It should also be noted that in a clinical setting longitudinal fractures commonly occur in endodontically treated teeth either with or without a post. The root canals of the sample teeth in the current study were not filled, which may have helped detection for both modalities.

Under the conditions of the experiment, however, LCT performed very well, with eight out of ten observers attaining A_z values between 0.9 and 1.0 and one observer reaching a value as high as 0.99. While one would expect near perfect performance when 180 basis projections are taken, this study revealed a number of issues with the technique. The images contained streaking artifacts in areas of reduced attenuation, such as the interproximal spaces in areas surrounding the embedded teeth. Streaking was less in adjacent teeth that were not taken out of the native alveolus and in areas in which wax provided additional attenuation. The use of the IRIS 2000 software for viewing the images in a multi-planar mode imposed two problems. Firstly, it was noticed that there was a loss of image quality when the images were converted from the raw format to GIPL format. Secondly, the software did not allow the observers to perform additional reslicing of the image volume, which in some cases significantly reduced the value of images in at least one of the planes.

While the current study has demonstrated the feasibility of detecting longitudinal fractures *in vitro*, translation into a clinical application cannot easily be accomplished at this point. The additional attenuation from soft and hard tissues tissue may reduce the streaking artifact problem, but also leads to fewer photons reaching the detector, which is known to reduce the signal-to-noise ratio. Clearly, the use of 180 conventional basis images for generating the image volume is unacceptable in a clinical situation. Further studies are required that focus on the dose aspects of LCT, addressing both detector efficiency and the minimum number of basis projections required to achieve high diagnostic accuracy. Based on the results of this study, it is concluded that LCT significantly improves the detection of longitudinal fractures *in vitro* compared to conventional periapical radiography.

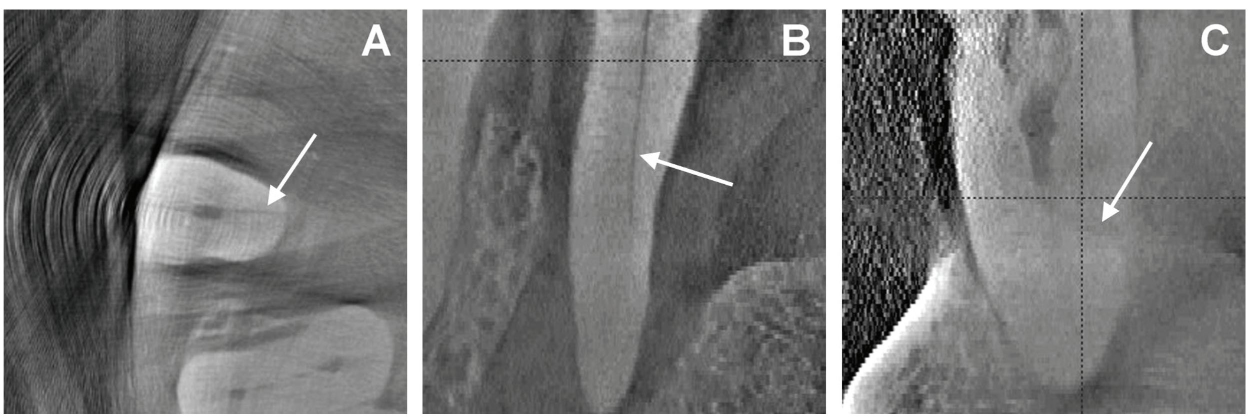

Figure 3. Multiplanar reconstruction views (MPR). Axial (A), Sagittal (B), Coronal (C). Arrows indicate fracture. Cross-hairs do not correspond to prevent the fracture to be obscured in the illustration.

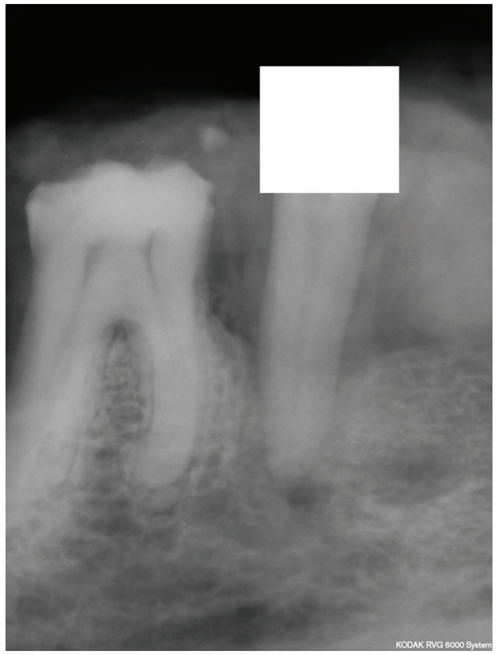

Figure 4. Conventional digital radiograph of the same tooth as in Figure 3.

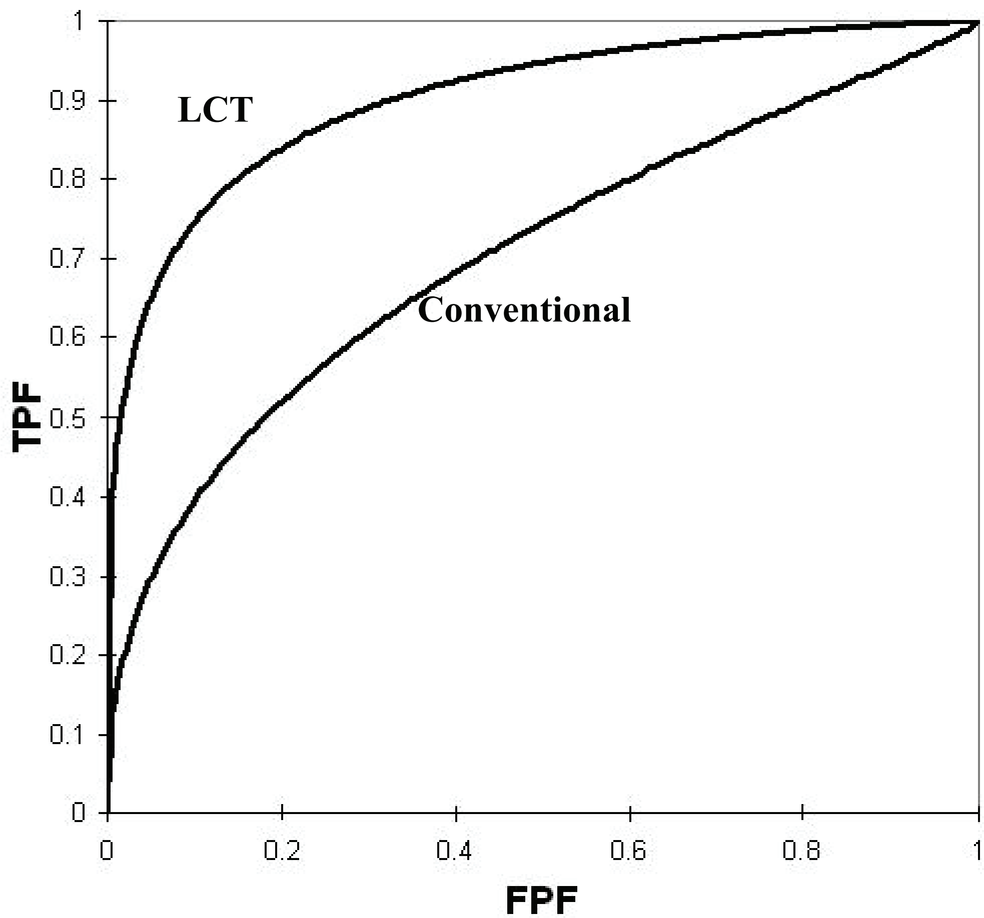

Figure 5. ROC curves for LCT (A_z=0.91) and conventional radiography (A_z=0.70) based on pooled data from all of observers. FPF: false positive fraction (1- specificity); TPF: true positive fraction (sensitivity).

Table 1. Sample

Teeth	Fractured	Non-fractured
Mandibular premolar	11	7
Maxillary premolar	6	6
Mandibular molar	8	7
Maxillary molar	5	10
Total	30	30

Table 2. Detection accuracy of Longitudinal Fractures as measured by Az (ROC analysis) for ten observers and the two modalities tested.

	LCT	Conventional
Observer	**Az**	**Az**
1	0.93	0.82
2	0.95	0.75
3	0.93	0.59
4	0.92	0.67
5	0.76	0.66
6	0.95	***
7	0.92	0.72
8	0.99	0.64
9	0.80	0.66
10	0.92	0.78
Mean	0.91	0.70
SD	0.07	0.07

***Missing Data. ANOVA. Observer: p =0.319 ; Modality: p = 0.0002

References

1. Tamse A, Fuss Z, Lustig J, Kaplavi J. An evaluation of endodontically treated vertically fractured teeth. *J Endod* 1999; **25:** 506-8.

2. Rivera EM, Williamson A. Diagnosis and treatment planning: cracked tooth. *Tex Dent J* 2003; **120:** 278-83.

3. Walton RE. Radiology and endodontics. *Oral surg Oral Med Oral Pathol Oral Radiol Endod* 1995; **80:** 495.

4. Walton RE. Longitudinal tooth fractures. In: Walton RE, Torabinejad M, (ed). *Principles and Practice of Endodontics.* Philadelphia: WB Saunders Company, pp 499-519.

5. Holcomb J, Pitts D, Nicholls J. Further investigation of spreader loads required to cause vertical root fracture during lateral condensation. *J Endod* 1987; 277-284.

6. Walton RE, Michelich RJ, Smith NG. The histopathogenesis of vertical root fractures. *J Endod* 1984; **10:** 48-56.

7. Schetritt A, Steffensen B. Diagnosis and management of vertical root fractures. *J Can Dent Assoc* 1995; **61:** 607-13.

8. Tamse A, Zilburg I, Halpern J. Vertical root fractures in adjacent maxillary premolars: an endodontic-prosthetic perplexity. *Int Endod J* 1998; **31:** 127-32.

9. Nair MK, Nair UDP, Gröndahl HG, Webber RL, Wallace JA. Detection of artificially induced vertical radicular fractures using tuned aperture computed tomography. *Eur J Oral Sci* 2001; **109:** 375-379.

10. Van Daatselaar A, Dunn S, Spoelder H, Germans D, Renambot L, Bal H, Van der Stelt P. Feasibility of Local CT of dental tissues. *Dentomaxillofac Radiol* 2003; **32:** 173-180.

11. Van Daatselaar A, Tyndall D, Van Der Stelt P. Detection of caries with local CT. *Dentomaxillofac Radiol* 2003; **32:** 235-241.

12. Monaghan P, Bajalcaliev JG, Kaminski EJ, Lautenschlager EP. A method for producing experimental simple vertical root fractures in dog teeth. *J Endod* 1993; **19:** 512-5.

13. Arai Y, Tammisalo E, Iwai K, Hashimoto K, Shinoda K. Development of a compact computed tomographic apparatus for dental use. *Dentomaxillofac Radiol* 1999; **28:** 245-248.

14. Ito K, Gomi Y, Sato S, Arai Y, Shinoda K. Clinical application of a new compact CT system to assess 3-D images for the preoperative treatment planning of implants in the posterior mandible. A case report. *Clin Oral Implants Res* 2001; **12:** 539-542.

15. Terakado M, Hashimoto K, Arai Y, Honda M, Sekiwa T, Sato H. Diagnostic imaging with newly developed ortho cubic super-high resolution computed tomography (Ortho-CT). *Oral Surg Oral Med Oral Pathol Oral Radiol Endod* 2000; **89:** 509-518.

MANUSCRIPT II

Effect of the number of basis images on the detection of longitudinal tooth fractures using Local Computed Tomography

Abstract

Objectives: To determine the effect of the number of basis images on the accuracy of Local CT in detecting longitudinal fractures and test the accuracy of terminal point assessment.

Methods: Longitudinal fractures were induced in 30 of 60 teeth. LCT volumes were generated from 180, 60, 36, and 20 basis images. Ten observers determined the presence of a fracture and its terminal point. ROC analysis and kappa statistics were used.

Results: A_z-values were 0.91, 0.84 , 0.74 , 0.57 and 0.70 for LCT180, LCT60, LCT36, LCT20 and conventional radiography, respectively (ANOVA: $p< 0.0001$). LCT180 and LCT60 outperformed the other modalities. The respective kappa values were 0.52, 0.40, 0.37, 0.16 and 0.32 (ANOVA: $p=0.00$). LCT180 and LCT60 provided better agreement.

Conclusions: LCT maintained its efficacy for detecting longitudinal fractures with 60 instead of 180 basis images. Agreement between actual and observed terminal point locations was moderate for LCT60 and LCT180.

INTRODUCTION

At present, it remains virtually impossible to detect non-displaced longitudinal fractures in a clinical setting. Radiographs are usually taken as part of the diagnostic work-up. However, the presence of a fracture can often only be confirmed after extraction of the tooth. Radiographic detection is highly dependent on the orientation of the fracture. The inability of conventional imaging modalities to adequately visualize longitudinal fractures indicates the need for the development and study of alternative diagnostic imaging systems that carry the potential of improving detection.[1]

Increasing the detection rate requires an imaging modality that delivers sufficient spatial resolution and is invariant to fracture orientation. Local Computed Tomography (LCT) offers an opportunity to meet these requirements. LCT uses a cone-beam x-ray geometry with a small field of view and a high-resolution detector. The feasibility of LCT for the detection of longitudinal fractures was previously demonstrated. The mean A_z value computed from receiver operating characteristic curves was 0.91. To achieve this high level of accuracy, 180 basis projections were used to generate the image volume. It was recognized that future clinical application of this modality would require a significant reduction in dose. One approach to achieving a lower dose is to reduce the number of basis projections. It has previously been shown that a significant reduction in the number of basis projections maintained the accuracy of LCT for detecting proximal caries lesions.[2] It is

Recognized, however, that the use of fewer basis images reduces signal strength and increases noise.

The purpose of the current study was to determine the effect of the number of basis images on the accuracy of Local CT in detecting longitudinal tooth fractures. In addition, the observers' ability to identify the terminal point of a fracture was assessed.

Materials and Methods

An *in vitro* model was used consisting of sixty extracted human teeth. Endodontic access openings were made and the canals were located. The roots of thirty of the teeth were placed in acrylic in order to prevent splitting of the roots. A screwdriver type wedge was placed in the canals and fractures were induced using controlled pressure applied by gentle tapping. In order to prevent the induction of a displaced fracture, the progression of the fracture was monitored by removing the tooth from the acrylic.[3] Teeth that presented one fracture along the long axis of the root were included in the study. The remaining thirty teeth served as controls. Each tooth was placed in a widened alveolus of an otherwise dentate dry mandible and held in place with boxing wax and orthosil (Orthosil Silicone Dental "Wax", DentaKit ™, Belmont, CA). Orthosil served as a surrogate for trabecular bone. A mixture of natural grains was mixed in the orthosil to simulate marrow spaces. The dry mandible was covered with boxing wax to simulate soft tissues.

Image acquisition

The *in vitro* LCT imaging system consisted of a conventional cone-beam dental x-ray source (Planmeca Prostyle Intra, Planmeca OY, Helsinki, Finland), an object stage and a high-resolution digital x-ray detector. All components were mounted on an optical rail with micro-positioning equipment (Spectra-Physics, Mountain View, CA). For ease of experimentation, the mandible was placed on a motorized rotator mounted on high-precision translators. A size-2 Schick CDR sensor served as the x-ray detector (Schick Technologies, Inc., Long Island City, NY). This detector is capable of producing images with a linear gray scale of 12 bits per pixel and has a pixel size of 40μm x 40μm. Careful calibration assured optimal alignment of the source, the object and the detector. Exposure settings were set at 70 kVp, 8 mA and 1.25 seconds. The source-to-object distance and object-to-sensor distance were fixed at 65 cm and 12.5 cm, respectively. 180 basis images were taken with one degree separation along an 180^{o} arc. From this image set, subsequent sets were compiled of 60, 36 and 20 basis images with 3^{o}, 5^{o} and 9^{o} separation, respectively. Image volumes were generated from the exported raw images using a filtered back projection reconstruction algorithm.[4] Five slices were averaged, thus generating axial slices with a thickness of 0.2 mm (5x40μm). Following conversion to GIPL (Guys Image Processing Lab) format, the image volume was displayed in a multi-planar reconstruction format using the IRIS 2000 software (Department of Computer Sciences, The University of North Carolina at Chapel Hill, Chapel Hill, NC). Figure 6 shows a single sagittal slice of the same tooth generated from different numbers of basis images.

Conventional intraoral radiographs were acquired immediately after each LCT scan using a Kodak RVG 6000 sensor (Eastman Kodak, Rochester, NY). In order to prevent the status of the crown to bias the observer's assessment of the root, the crowns of the teeth were blocked out. For LCT this was accomplished by deleting the axial slices that included the crown of the experimental tooth. For conventional radiography, an opaque rectangular mask was overlaid onto the crowns. Figure 7 shows a masked conventional radiograph of the same tooth as in Figure 6.

Observation sessions

Ten observers were recruited: 4 radiologists, 1 radiology resident, 4 endodontic residents, and 1 periodontist. The observers reviewed images from five modalities: four LCT variants (180, 60, 32 and 20 basis images) and one conventional. The observations were spread over a total of nine sessions. One session consisted of 60 conventional intraoral images and eight sessions were used to review the LCT images, 30 at the time. All LCT images were combined and randomized. Half the observers viewed the conventional images first, the other half started with the LCT images. All images were displayed on a 21.3 inch true color flat panel monitor (Samsung, Sync Master 213T, Samsung Electronics co., ltd, Ridgefield Park, NJ) at its native resolution of 1600x1200 pixels under dimmed ambient lighting. Conventional images were presented as a stack using ImageJ against a black background. LCT images were presented in IRIS 2000. By clicking a location of interest in any one of the planes, the observer was able to align the three planes at any point.

The observers assessed the presence or absence of a longitudinal fracture and recorded their response on a 5-point probability scale as follows: 1=fracture definitely not present; 2=fracture probably not present; 3=unsure; 4=fracture probably present; 5=fracture definitely present. If the response was either 4 or 5 (fracture probably or definitely present), the observers were asked to assess the terminal point of the fracture. The terminal point was defined as the most apical location of the fracture. For this purpose, the root was divided subjectively in coronal, middle and apical thirds. Receiver Operating Characteristic (ROC) curves were constructed for each observer and each modality using the ROCKIT software (Version 0.9, Charles E Metz, The University of Chicago, Chicago, IL).

Ground truth

Following air drying, the teeth were stained with 1% methylene blue. The dye was placed in the canal and allowed to flow through the fracture if present. The presence of fractures and terminal points was assessed visually by a single person. The absence of fractures in the control teeth was also confirmed through this process.

Statistical analysis

Differences between the areas under the ROC curves (A_z) were analyzed with ANOVA to test the null–hypothesis of no difference between the imaging modalities and the observers. Tukey's HSD test was used for post-hoc analysis. Concordance between the terminal points selected by the observers and the actual location of the terminal points was expressed by Cohen's kappa. Differences between the kappa values were tested for statistical significance using ANOVA and Tukey's HSD.

Results

Table 3 shows the A_z values from the ROC analysis by observer and by modality. The highest mean A_z (0.91) was obtained for LCT using 180 basis images, whereas the lowest A_z was found for LCT using 20 basis images (mean A_z = 0.57). Conventional radiography with a mean A_z of 0.70 performed better than LCT with 20 basis images. Figure 8 shows the ROC curves for all the modalities based on pooled data from all the observers. The analysis of variance showed that there was a statistically significant difference between the modalities ($p< 0.0001$) and between the observers ($p= 0.01$). Homogeneous subsets were identified based on Tukey's HSD test. LCT with 180 and 60 basis images were not statistically different form one another. LCT with 36 basis images and conventional radiography were also not statistically different from one another, however, both modalities were statistically different from LCT with 180 and 60 basis images. LCT with 20 basis images was inferior to any of the other modalities. Although ANOVA identified a significant difference between the observers, Tukey's HSD test grouped all observers as one homogeneous subset.

The concordance between the observers' assessment of the location of the terminal point and the actual location are shown in Table 4. The kappa values indicate slight concordance for LCT20, fair concordance for conventional radiography and LCT36 and moderate concordance for LCT60 and LCT180.[5] Differences between the modalities were statistically significant (ANOVA: p=0.00). Differences between the observers were not statistically significant (ANOVA: p=0.24). Tukey's HSD identified three homogeneous subsets: (1) Conventional and LCT20; (2) Conventional, LCT36 and LCT60 and (3) LCT60 and LCT180.

Discussion

The capability of radiographic imaging in dentistry has experienced a dramatic expansion with the introduction of cone-beam CT (CBCT). The increase in the quantity and quality of radiographic information obtained through CBCT has come with only a modest increase in patient dose in comparison to traditional radiographic imaging modalities. In many cases, this increase in dose is justified for the information gained. However, there is also a growing concern that CBCT examinations are ordered when other types of modalities imparting a lower dose to the patient would suffice. The proliferation of CBCT scanners in the dental field raises the concern that the dose to the dental population may increase without an equally large increase in the diagnostic, treatment and outcome efficacies.

Dose issues become more problematic when an increase in the signal-to-noise ratio and spatial resolution is sought. Generally, a greater photon flux is required to achieve better image quality. This issue has become apparent in the development of Local CT (LCT). LCT has shown to be highly efficacious, but the dose required to achieve such efficacy, as inferred from the number of basis images, would not be acceptable in a clinical setting. As initial studies have demonstrated the feasibility of LCT, it has become relevant to explore approaches for reducing dose while maintaining diagnostic efficacy. One such approach is to reduce the number of basis images for generating the image volume. In a previous study it was suggested that 14-20 basis images were sufficient to maintain the accuracy in detecting proximal caries.[2]

In the current study, assessing the efficacy of detecting longitudinal fractures, an image volumes based on 20 basis images were inferior to those based on 36 images or more and also inferior to conventional periapical radiography. Although a small decrease in the A_z value was observed, a reduction in the number of basis images from 180 to 60 did not result in a statistically significant difference in diagnostic accuracy. This suggests that a considerable reduction in dose can be achieved through this mechanism. LCT based on 36 basis images was not statistically different from conventional radiography. The difference between this result and the results obtained by Van Daatselaar and coworkers may be explained by differences in experimental factors. However, it is conceivable that the potential for basis image reduction is task dependent. The lower sampling rate leads to decreased signal strength mainly through a reduction in contrast with a concurrent increase in noise. One of the manifestations of the increase in noise is the amplification of streaking artifacts. In the case of longitudinal fractures, the signal and noise share common features, thus making signal detection more difficult.

It may be argued that when the number of basis images is being reduced to a level that is less conducive for the CT back projection algorithm, a different image acquisition geometry and image reconstruction technique may become superior. It is at this level that LCT and tuned aperture computed tomography (TACT®) blend, both being imaging modalities on a sampling continuum.[6] The utility of TACT for the detection of traumatic root fractures in anterior teeth has previously been demonstrated.[1, 7-9] As the strength of the signal to be detected is reduced, whether it being lower in contrast or smaller in size, the sampling rate needs to increase and LCT may become the preferred technique. Further studies are required to test this hypothesis. Future studies are also planned to test alternative approaches to reducing dose, including further development of the reconstruction algorithm to reduce noise and artifacts. The ongoing development of x-ray detectors will also help to bring the clinical application of LCT closer.

Based on the results of this study it can be concluded that LCT maintains its efficacy for detecting longitudinal fractures with 60 instead of 180 basis images. A subsequent reduction to 36 basis images significantly reduced the detection rate. Observer assessment of the terminal point location showed moderate agreement with the actual location for LCT with 60 and 180 basis images.

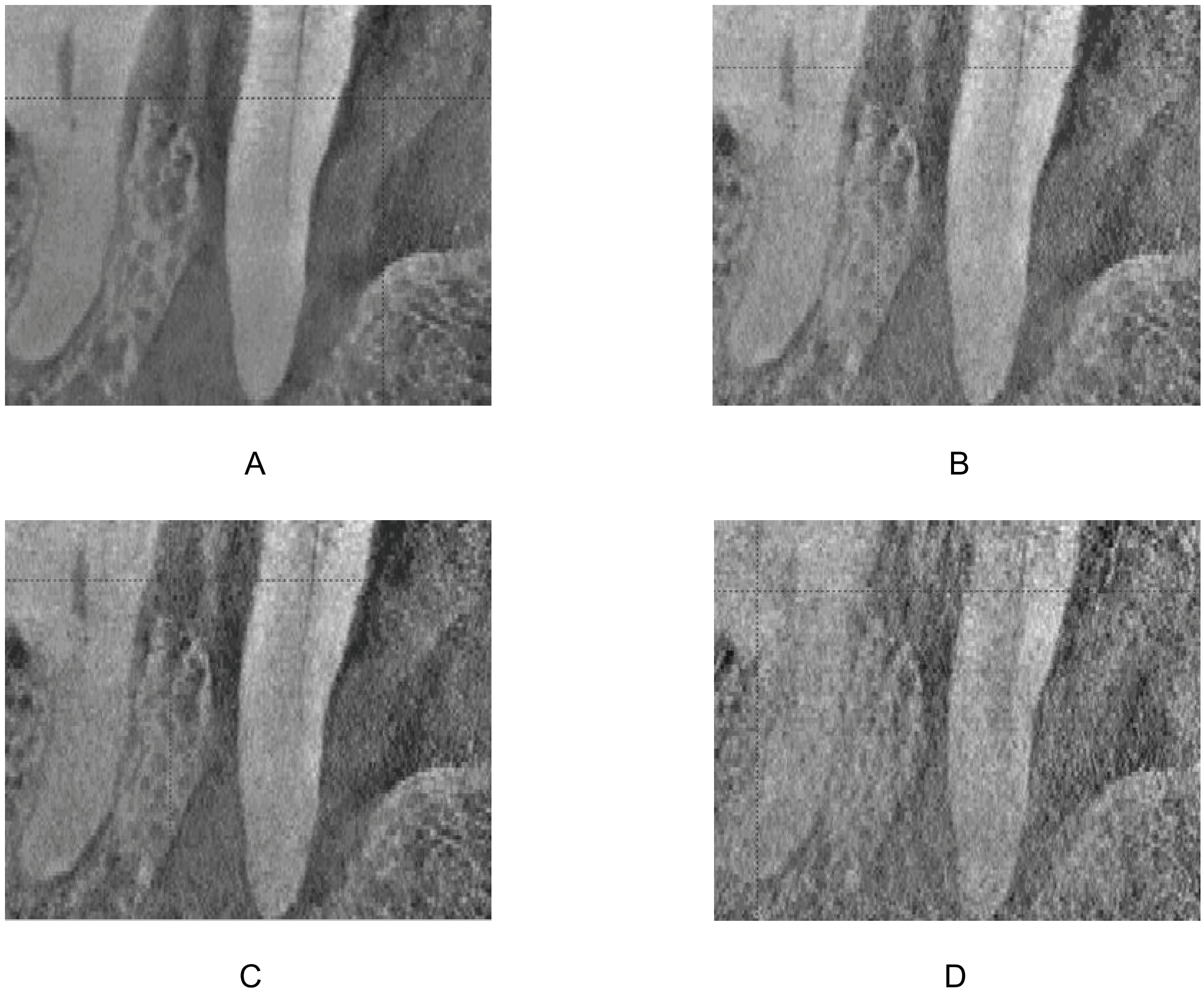

Figure 6. Local CT sagittal slices of the same tooth created with different number of basis images: 180 (A), 60 (B), 36 (C) and 20 (D).

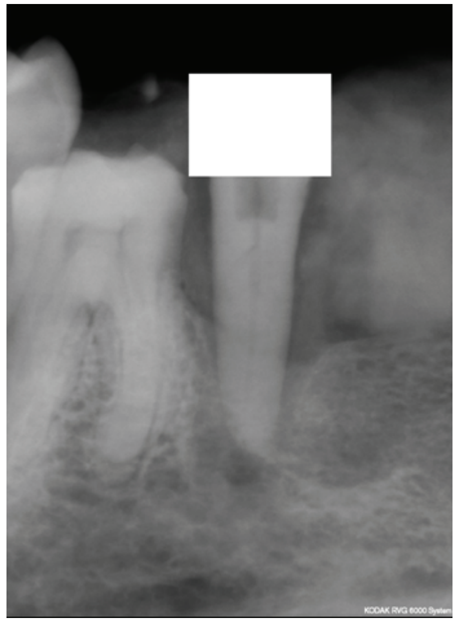

Figure 7. Conventional digital radiograph of the same tooth as in Figure 6.

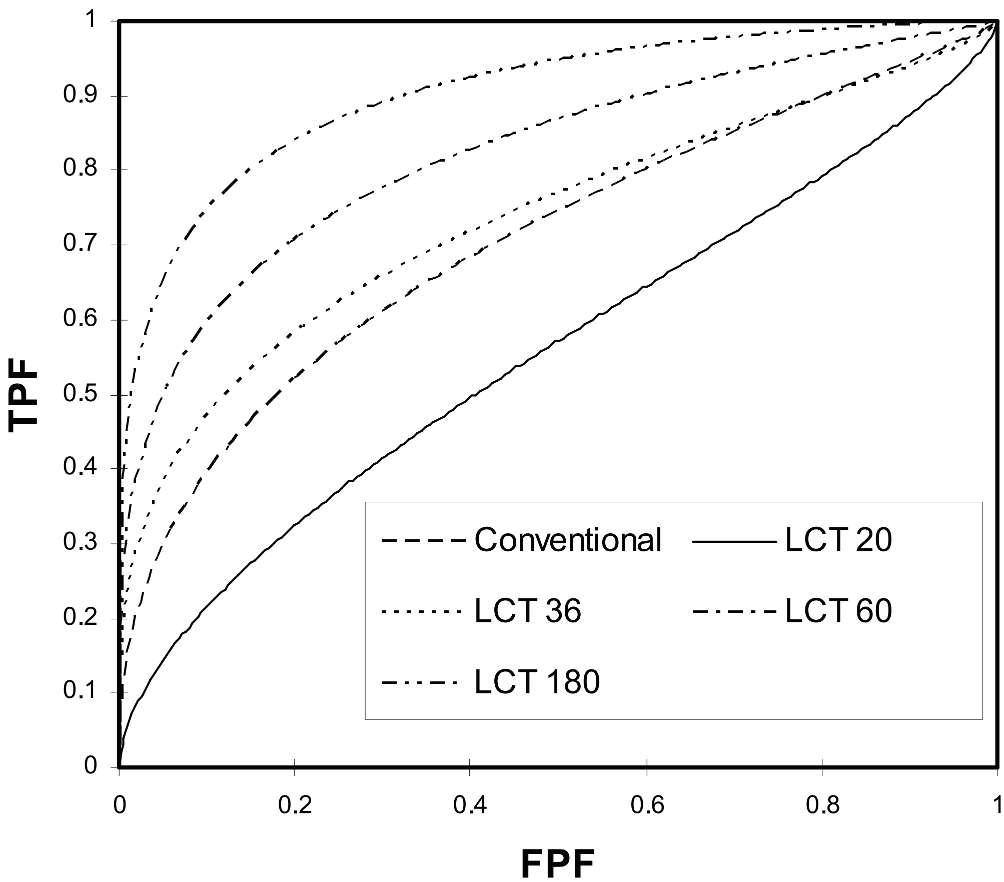

Figure 8. ROC curves of pooled data from all observers and all modalities

Table 3. Longitudinal fracture detection accuracy as measured by A_z (ROC analysis)						
Observer	CON	LCT20	LCT36	LCT60	LCT180	Homogeneous subsets
1	0.82	0.58	0.75	0.83	0.93	A
2	0.75	0.64	0.86	0.87	0.95	A
3	0.59	0.48	0.66	0.79	0.93	A
4	0.67	0.54	0.63	0.86	0.92	A
5	0.66	0.63	0.74	0.78	0.76	A
6	*	0.61	0.78	0.90	0.95	A
7	0.72	0.60	0.70	0.88	0.92	A
8	0.64	0.69	0.83	0.96	0.99	A
9	0.66	0.54	0.75	0.69	0.80	A
10	0.78	0.36	0.71	0.79	0.92	A
Mean	0.70	0.57	0.74	0.84	0.91	
SD	0.07	0.09	0.07	0.08	0.07	
Homogeneous subsets	A	B	A	C	C	

CON: Conventional radiography; LCT20: 20 basis images; LCT36: 36 basis images; LCT60: 60 basis images; LCT180: 180 basis images. ANOVA: Observer: $p=0.01$; Modality: $p<0.0001$. Homogeneous subsets from Tukey's HSD: $p<0.05$. *missing data.

Table 4. Linearly weighted kappa values representing the concordance between observers and ground truth regarding the location of the terminal point of the fracture

Observer	CON	LCT20	LCT36	LCT60	LCT180	Mean	SD
1	0.37	0.18	0.32	0.42	0.63	0.38	0.16
2	0.21	0.22	0.42	0.35	0.67	0.37	0.19
3	0.53	-0.01	0.26	0.24	0.56	0.32	0.23
4	0.19	0.19	0.24	0.56	0.52	0.34	0.18
5	0.15	0.14	0.17	0.22	0.30	0.20	0.07
6	0.40	0.28	0.53	0.50	0.62	0.47	0.13
7	0.28	0.19	0.35	0.46	0.44	0.35	0.11
8	0.40	0.25	0.61	0.65	0.54	0.49	0.16
9	0.30	0.11	0.28	0.21	0.36	0.25	0.10
10	0.32	0.06	0.51	0.35	0.58	0.36	0.20
Mean	0.32	0.16	0.37	0.40	0.52		
SD	0.11	0.09	0.14	0.15	0.12		
Homogeneous subsets	A/B	A	B	B/C	C		

CON: Conventional radiography; LCT20: 20 basis images; LCT36: 36 basis images; LCT60: 60 basis images; LCT180: 180 basis images. ANOVA: Observer: $p=0.24$; Modality: $p=0.00$. Homogeneous subsets from Tukey’s HSD: $p<0.05$.

References

1. Nair MK, Nair UDP, Gröndahl HG, Webber RL, Wallace JA. Detection of artificially induced vertical radicular fractures using tuned aperture computed tomography. *Eur J Oral Sci* 2001; **109:** 375-379.

2. Van Daatselaar AN, Van der Stelt PF, Weenen J. Effect of number of projections on image quality of local CT. *Dentomaxillofac Radiol* 2004; **33:** 361-9.

3. Monaghan P, Bajalcaliev JG, Kaminski EJ, Lautenschlager EP. A method for producing experimental simple vertical root fractures in dog teeth. *J Endod* 1993; **19:** 512-5.

4. Van Daatselaar A, Dunn S, Spoelder H, Germans D, Renambot L, Bal H, Van der Stelt P. Feasibility of Local CT of dental tissues. *Dentomaxillofac Radiol* 2003; **32:** 173-180.

5. Landis JR, Koch GG. The measurement of observer agreement for categorical data. *Biometrics* 1977; 159-174.

6. Webber RL, Horton RA, Tyndall DA, Ludlow JB. Tuned-aperture computed tomography (TACT). Theory and application for three-dimensional dento-alveolar imaging. *Dentomaxillofac Radiol* 1997; **26:** 53-62.

7. Nair MK, Gröndahl HG, Webber RL, Nair UP, Wallace JA. Diagnostic accuracy of Tuned Aperture Computed Tomography (TACT). *Swed Dent J Suppl* 2003; **96:** 1-93.

8. Nair MK, Gröndahl HG, Webber RL, Nair UP, Wallace JA. Effect of iterative restoration on the detection of artificially induced vertical radicular fractures by Tuned Aperture Computed Tomography. *Oral Surg Oral Med Oral Pathol Oral Radiol Endod* 2003; **96:** 118-25.

9. Nair MK, Nair UP, Gröndahl HG, Webber RL. Accuracy of tuned aperture computed tomography in the diagnosis of radicular fractures in non-restored maxillary anterior teeth--an in vitro study. *Dentomaxillofac Radiol* 2002; **31:** 299-304.

Discussion and Conclusions

The introduction of 3D cone-beam CT has dramatically changed the diagnostic capabilities in dentistry. 3D images can be generated at relatively low doses and with high resolution compared to conventional CT. Recognizing the high resolution requirements for oral and maxillofacial applications, a cone-beam CT system was developed with a smaller field of view.[48, 50, 51] Van Daatselaar and coworkers took this concept one step further by using a high-resolution intraoral sensor as the image detector. Their studies demonstrated the feasibility of Local CT (LCT) and its ability to improve caries detection relative to conventional radiography.[46, 52] While still in its infancy and with many problems remaining to be solved, demonstrating the feasibility of LCT for solving other diagnostic problems has become a driving force behind its further development. The detection of longitudinal fractures represented a suitable and clinically relevant diagnostic problem in this regard.

This study demonstrated that LCT provided a significant improvement in the accuracy of detecting longitudinal fractures compared to periapical radiographs. While the comparison to conventional radiography appears unfair, the use of conventional radiographs in this study served to demonstrate that detection of the fractures represented a true challenge to the observers. It was noted that for most observers, the A_z values for conventional radiography were not as low as expected, with a positive outlier as high as 0.82. This implies that longitudinal fractures actually do result in detectable radiographic signs or that the *in vitro* model was not an ideal simulation of the actual clinical world. Limitations of the model included the method of fracture induction and the environment in which the teeth were placed. The fact that there was no real bone surrounding the tooth and the lack of periodontal ligament (PDL) may have played a role in enhancing fracture visibility in conventional radiographs. It was learned from the pilot study that a significant increase in noise and decrease in contrast occurred in the subsequent imaging of a single tooth, a jaw segment and, finally, an entire mandible. While the results are promising, many other factors have to be taken into account as patient volumes, movement of the patients and possible artifacts that can be created from metallic restorations need to be considered in further development of this modality. In a clinical setting, for example, longitudinal fractures commonly occur in endodontically treated teeth either with or without a post. The root canals of the sample teeth in the current study were not filled, which may have helped detection of fractures for both modalities.

Under the conditions of the experiment, however, LCT performed very well, with eight out of ten observers attaining A_z values between 0.9 and 1.0 and one observer reaching a value as high as 0.99. While one would expect near perfect performance when 180 basis projections are taken, this study revealed a number of issues with the technique. The images contained streaking artifacts in areas of reduced attenuation, such as the interproximal spaces in areas surrounding the embedded teeth. Streaking was less in adjacent teeth that were not taken out of the native alveolus and in areas in which wax provided additional attenuation. The use of the IRIS 2000 software for viewing the images in a multi-planar mode imposed two problems. Firstly, it was noticed that there was a loss of image quality when the images were converted from the raw format to GIPL format. Secondly, the software did not allow the observers to perform additional reslicing of the image volume, which in some cases significantly reduced the value of images in at least one of the planes.

While the current study has demonstrated the feasibility of detecting longitudinal fractures *in vitro*, translation into a clinical application cannot easily be accomplished at this point. The additional attenuation from soft and hard tissues tissue may reduce the streaking artifact problem, but also leads to fewer photons reaching the detector, which is known to reduce the signal-to-noise ratio.

Dose issues become more problematic when an increase in the signal-to-noise ratio and spatial resolution is sought. Generally, a greater photon flux is required to achieve better image quality. This issue has become apparent in the development of Local CT (LCT). LCT has shown to be highly efficacious, but the dose required to achieve such efficacy, as inferred from the number of basis images, would not be acceptable in a clinical setting. As initial studies have demonstrated the feasibility of LCT, it has become relevant to explore approaches for reducing dose while maintaining diagnostic efficacy. One such approach is to reduce the number of basis images for generating the image volume. In a previous study it was suggested that 14-20 basis images were sufficient to maintain the accuracy in detecting proximal caries.[47]

In the current study, assessing the efficacy of detecting longitudinal fractures, an image volumes based on 20 basis images were inferior to those based on 36 images or more and also inferior to conventional periapical radiography. Although a small decrease in the A_z value was observed, a reduction in the number of basis images from 180 to 60 did not result in a statistically significant difference in diagnostic accuracy. This suggests that a considerable reduction in dose can be achieved through this mechanism. LCT based on 36 basis images was not statistically different from conventional radiography. The difference between this result and the results obtained by Van Daatselaar and coworkers may be explained by differences in experimental factors. However, it is conceivable that the potential for basis image reduction is task dependent. The lower sampling rate leads to decreased signal strength mainly through a reduction in contrast with a concurrent increase in noise. One of the manifestations of the increase in noise is the amplification of streaking artifacts. In the case of longitudinal fractures, the signal and noise share common features, thus making signal detection more difficult.

It may be argued that when the number of basis images is being reduced to a level that is less conducive for the CT back projection algorithm, a different image acquisition geometry and image reconstruction technique may become superior. It is at this level that LCT and tuned aperture computed tomography (TACT®) blend, both being imaging modalities on a sampling continuum.[37] The utility of TACT for the detection of traumatic root fractures in anterior teeth has previously been demonstrated.[24, 25, 53] As the strength of the signal to be detected is reduced, whether it being lower in contrast or smaller in size, the sampling rate needs to increase and

LCT may become the preferred technique. Further studies are required to test this hypothesis. Future studies are also planned to test alternative approaches to reducing dose, including further development of the reconstruction algorithm to reduce noise and artifacts. The ongoing development of x-ray detectors will also help to bring the clinical application of LCT closer.

If Local CT is going to be further developed, studies have to be carried out in order to show the capability of this setup of imaging *in vivo* patients and to quantify the amount of resolution required by a system to produce diagnostically meaningful images. Other than the detection of longitudinal fractures, this modality can provide information of structures that cannot be visualized entirely. Research can be focused on different applications of this setup, such as the assessment of root canal morphology, periodontal disease to assess bone loss at the level of the crest or periapical areas. This modality not only can aid in the detection of pathology in 3D but also may help reduce and/or eliminate invasive surgical exploration.

Even though LCT is a promising technology, the cost-benefit ratio has to be improved. Exploration of ways to improve image quality is necessary and it is expected that with the development of higher efficiency detectors to improve image quality at a lower dose.

Conclusions

- LCT significantly improves the detection of longitudinal fractures *in vitro* compared to conventional periapical radiography.

- LCT maintains its efficacy for detecting longitudinal fractures with 60 instead of 180 basis images.
- A subsequent reduction to 36 basis images significantly reduced the detection rate.
- Observer assessment of the terminal point location showed moderate agreement with the actual location for LCT with 60 and 180 basis images.

Appendix I:

Induction of Fractures

- Teeth were sterilized using Ethylene oxide
- The sample remained hydrated (water) at all times
- Roots were covered with wax and placed in acrylic blocks

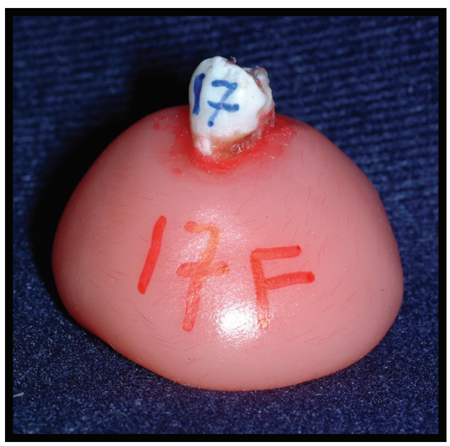

Figure 9. Tooth embedded in the acrylic block.

- Endodontic access openings were generated in the entire sample
- A wedge-shaped mini screwdriver was placed in the canal to generate fractures in 30 of the 60 teeth
    - Intermittent pressure was applied until the wedge became lodged in the canal
    - Direct visualization could be achieved by being able to remove the tooth from the acrylic block

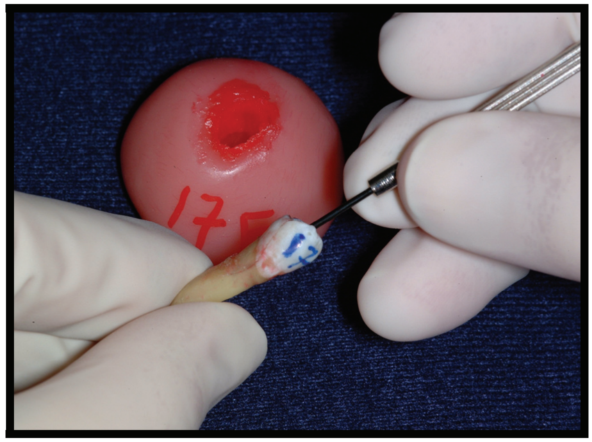

Fig. 10. Visualization of the extent of the fracture in order to control the size.

- Single non-displaced longitudinal fractures were included in the sample
    - Teeth with multiple fractures were excluded from the fractured group
- The control group was had access openings, but no fractures (30 of the 60 teeth)
- The water in the containers where the samples were kept was replaced on a weekly basis

Appendix II:

LCT Setup

- The setup consisted of an optical rail with the following components:
    - Intraoral x-ray unit (Prostyle Intra, Planmeca USA, Roselle, IL)
        - Operated at :
            - 70 kVp
            - 8 mA
            - 1.25 seconds
    - Lead Collimator
    - Motorized rotating stage (Newport Corporation-Oriel Products, Stratford, CT)
        - Adjustment in the vertical and horizontal aspect could be done in order to:
            - Calibrate the unit
            - Position the teeth
    - Size-2 CMOS sensor (Schick CDR, Schick Technologies, Inc., Long Island City, NY)
        - 12 bit linear gray scale
        - Size of outer sensor: 43x30 mm
        - Size of sensor active area: 36x25.6 mm

- Size of sensor thickness: less than 5 mm
- Signal-to-noise ratio: 120:1

- Position parameters
  - Source-Object-Distance: 65 cm
  - Object-Sensor-Distance: 12.5 cm
  - Source-Collimator: 54.5 cm

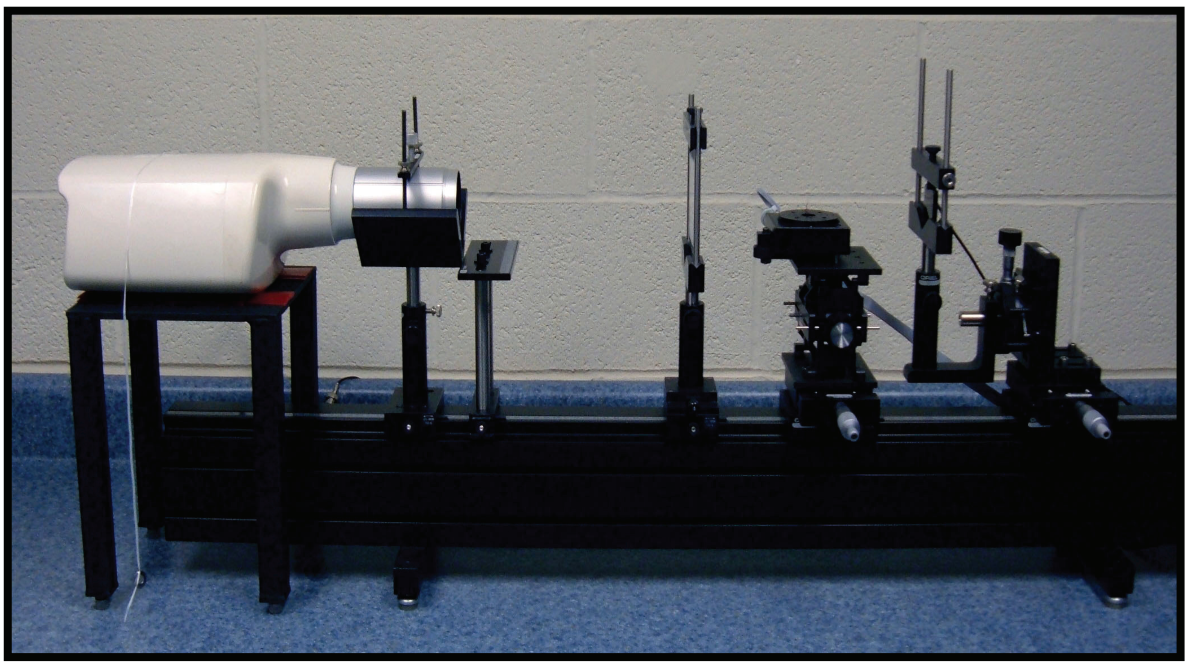

Figure11. Image of the LCT setup.

Appendix III:

Calibration of the Setup

- Orthogonal positioning of elements on the optic rail
- Vertical alignment of the following components was achieved:
    - Focal spot
    - Center of sensor
    - Center of collimator
- Parallel alignment of sensor columns with axis of rotation
    - A rod was placed on the rotating stage
    - The edges of the rod served as vertical references
    - Pseudo colorization was applied using the CDR software
    - An edge was selected and zoomed in
        - If the sensor was aligned, the entire columns remained the same color throughout the image
    - Rotation of sensor
        - clockwise or counterclockwise
            - According to the position of the sensor

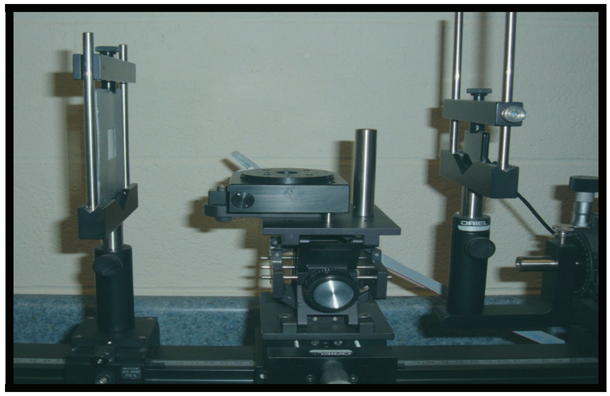

Figure 12. Rod mounted on the rotating stage

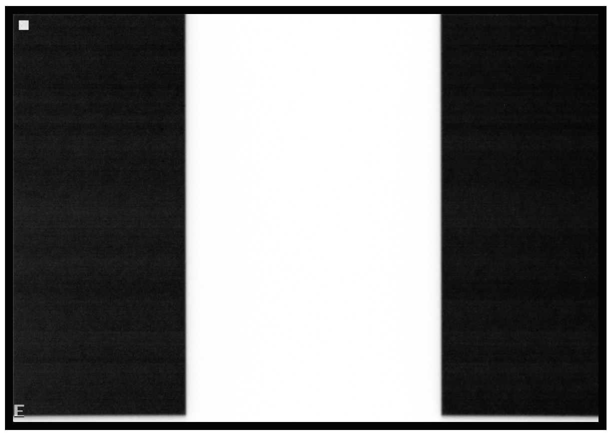

Figure13. Radiograph of the rod on the rotating stage

Figure 14. Pseudo-colorization of rod in the radiograph. CDR Schick software was used for this purpose.

- Horizontal alignment of focal spot and center of rotation
  - Placement of small rod
  - Translation of sensor stage
  - Symmetrical superimposition

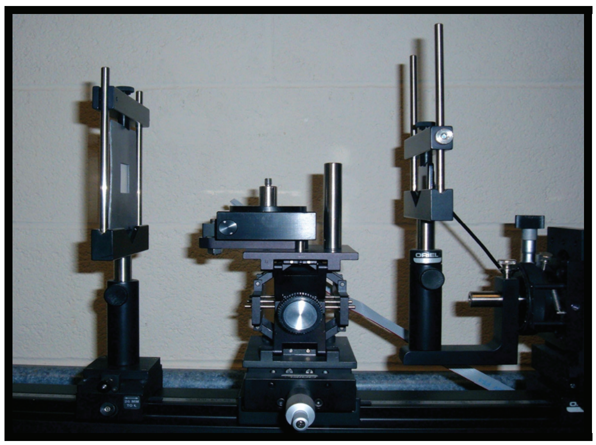

Figure 15. Small rod placed on rotating stage in front of the large rod.

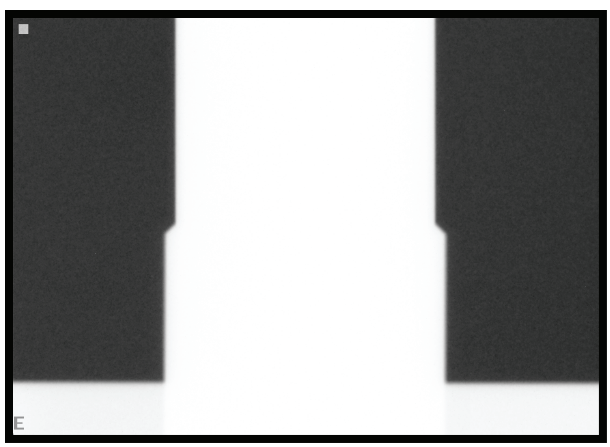

Figure16. Radiograph of rods and rotating table.

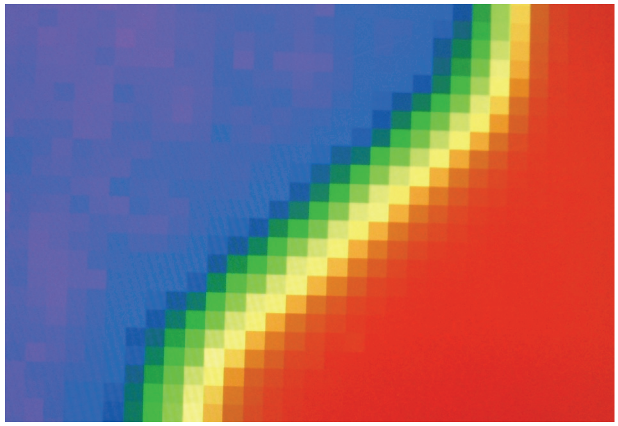

Figure 17. Pseudo colorized image. Pixels were counted on both sides of the rods until an equal number of pixels were achieved.

- Horizontal alignment axis of rotation and sensor
    - Course alignment
        - Approximation of left and right measurements
        - Translation of sensor to achieve this position
    - Fine alignment
        - An endodontic file was used for this step
        - A first image was taken at 0^0 using the CDR software
        - The rotation stage was rotated 180^0
        - A second image was taken at 180^0
        - Images were exported to Image J (Wayne Rasband, National Institutes of Health, USA)
        - Digital subtraction was applied
        - Translation of sensor stage
            - Until ideal alignment

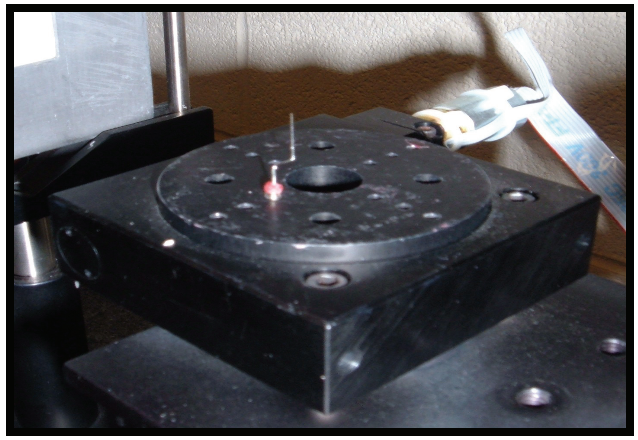

Figure 18. Image of the file on the rotating stage at 0^0.

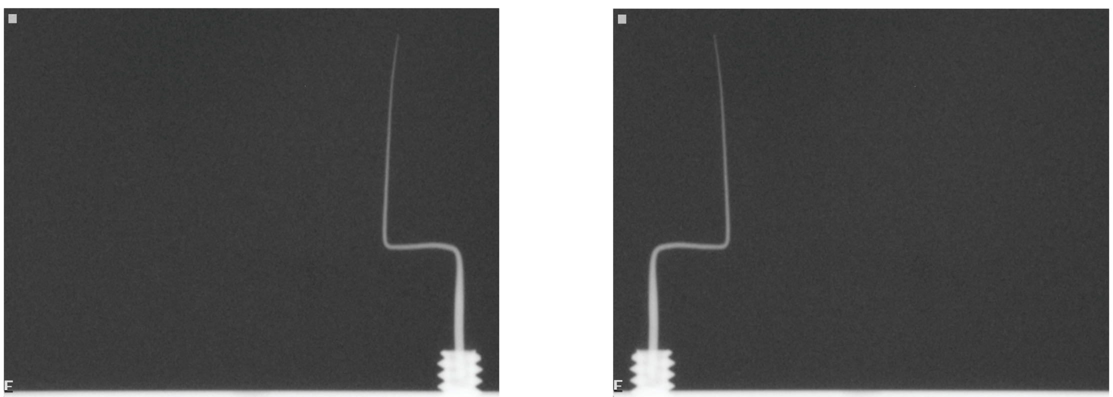

Figure 19. Radiograph of file at 0^0 and 180^0. Note that the superior aspect of the rotating stage was imaged and also served as reference for the alignment.

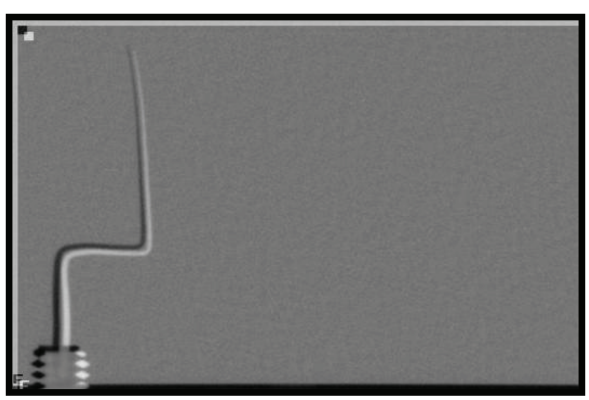

Figure 20. Image demonstrating lack of fine alignment after digital subtraction is applied.

Figure 21. Digital subtraction resultant image after fine alignment.

APPENDIX IV:

Image Acquisition

- Image acquisition was automated:
  - Exposure control
    - Software written by Oliver Monbureau, Electronics Technician, UNC School of Dentistry
    - The "delay" period allowed the tube to cool down before the next exposure
    - The "exposure" setting was set in a way that the exposure control would be sustained for the entire 1.25 seconds
  - Rotation stage
    - MVP Demo Version 1.4
    - 180 basis images were acquired by rotating the stage 1^0 after each exposure
  - Image capture
    - Schick CDR software
    - 12 bit linear
    - A mount of 180 images was created for each scan

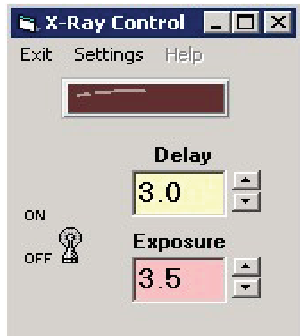

Figure 22. Exposure control interface.

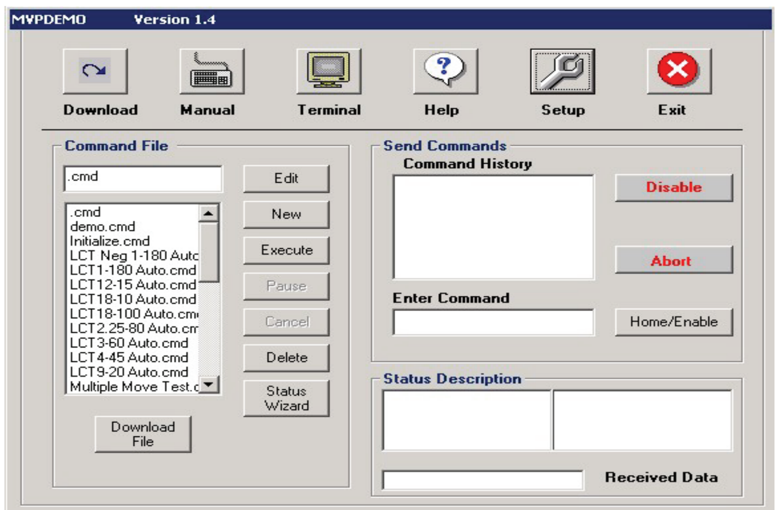

Figure 23. Rotating stage software control.

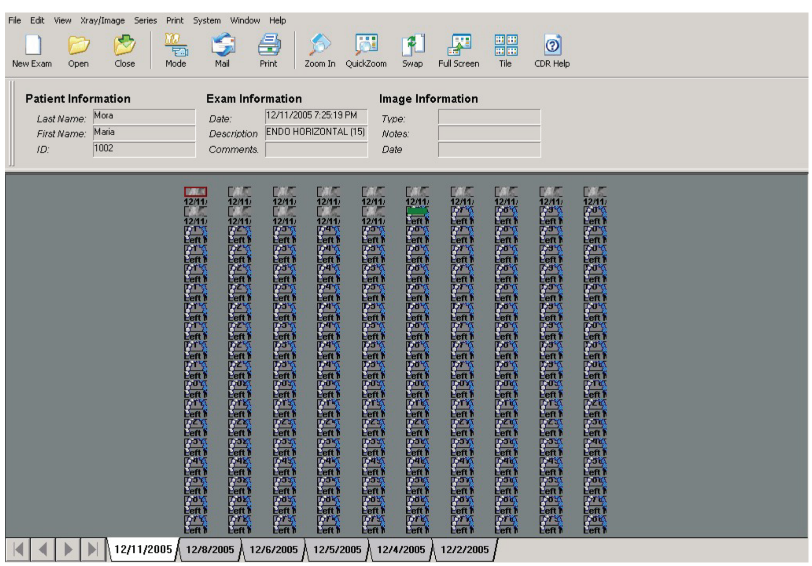

Figure 24. CDR Schick software. Mount of 180 images.

Appendix V:

Image Reconstruction

- Images were exported from the CDR Schick Data Administration Utility to ImageJ as 16 bit DICOM images
- Once the DICOM images were in ImageJ, they were converted to .raw images using a batch converter plug-in
- The 180 .raw images were opened using a raw file opener as 16 bit unsigned images
- The 180 images were converted into a stack and, using the bite swapper (Image J, Wayne Rasband, 2001) plug-in, the bites were swapped
- The resultant images were saved as an image sequence with .raw extension
- A batch file was created to rename the .raw images to .buf
- Another batch file was used to apply the backprojection algorithm where a set of parameters were selected including:
    - Image width- 900
    - Image height- 641
    - Slice width- 600
    - Slice height- 600
    - Number of projections- 180
    - Slice averaging- 5

    - Filters- Ramp filter and Hamming filter
- After reconstruction, the images were saved as .gif
- With ImageJ the reconstructed images were opened and converted into a stack
- Then the LUT was inverted for the entire stack of images

Appendix VI:

Pilot Study

The pilot study was divided in two parts:

1. Using a single tooth
    - Demonstrate the feasibility of the setup
        - Projection geometry parameters
        - Basic reconstruction algorithm
2. Using a segment of a mandible
    - To test shifting of pixels
    - To test filters to be applied in the reconstruction algorithm

Part I- Single tooth:

- Consisted of a single molar positioned in the center of rotation held to a base with wax
- The fracture was induced as explained in appendix A
- Imaging parameters were the same for this part with exception of the exposure time, which was 1.0 sec
- 180 basis images were taken with 1^0 separation

- Image reconstruction was done in the same manner as for the sample using a filtered back projection
- For this part only feasibility of acquiring images was assessed

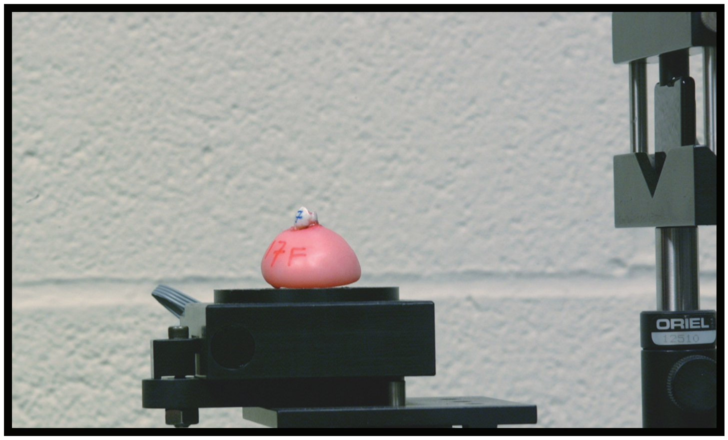

Figure 25. Single tooth on rotating table

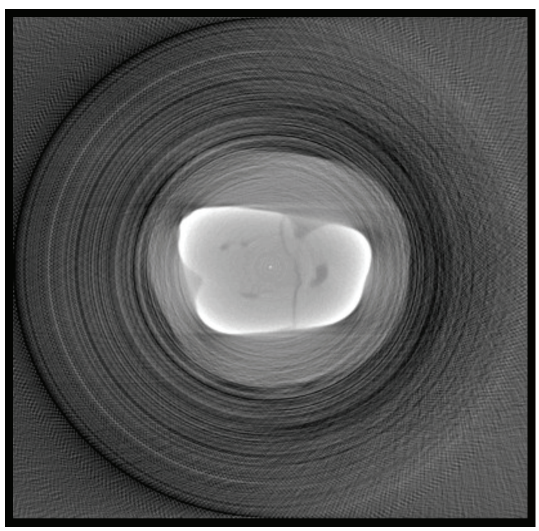

Figure 26. Axial view of fractured molar

Part II- Jaw segment:

- Image acquisition and reconstruction parameters for the baseline images were taken as for the single tooth
- A jaw segment was placed on the rotating stage and wax was added to the bony surfaces to simulate soft tissue

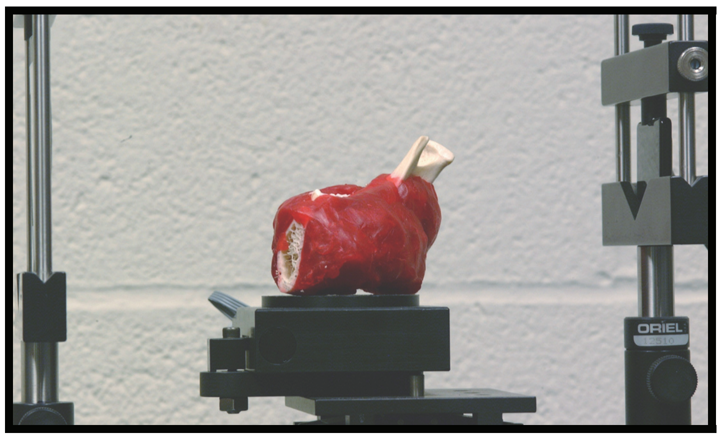

Figure 27. Jaw segment on rotating stage during scanning.

- For this part several parameters were tested:
    - Pixel shifting
        - Pixels were shifted 1,2,3,4,5 both positive and negatively
    - Filters- the reconstruction algorithm set at the beginning used a ramp filter and a hamming filter. Other combinations of filters were tested as variants to the ones selected previously
        - Ramp filter and Welch filter
        - Only applying the ramp filter
        - Applying the ramp filter and 50% cutoff

- Applying the ramp filter and 80% cutoff
- No high-pass filter

- Averaging of slices
  - Averaging 3 slices
  - Averaging 5 slices

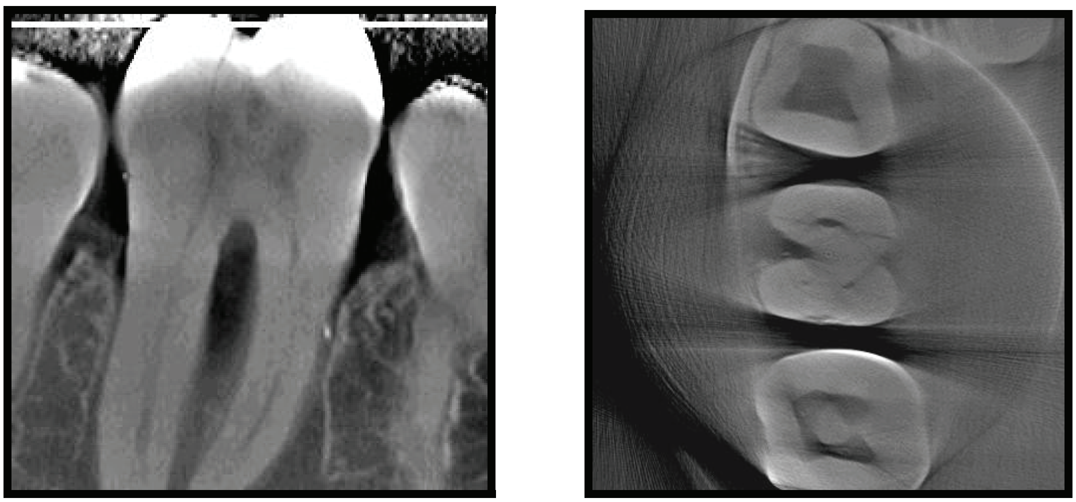

(A) (B)

Figure 28. Coronal view of molar in a jaw segment (A) notice the longitudinal fracture running parallel to the canal; (B) axial view of the same tooth.

Appendix VII:

ROC curves

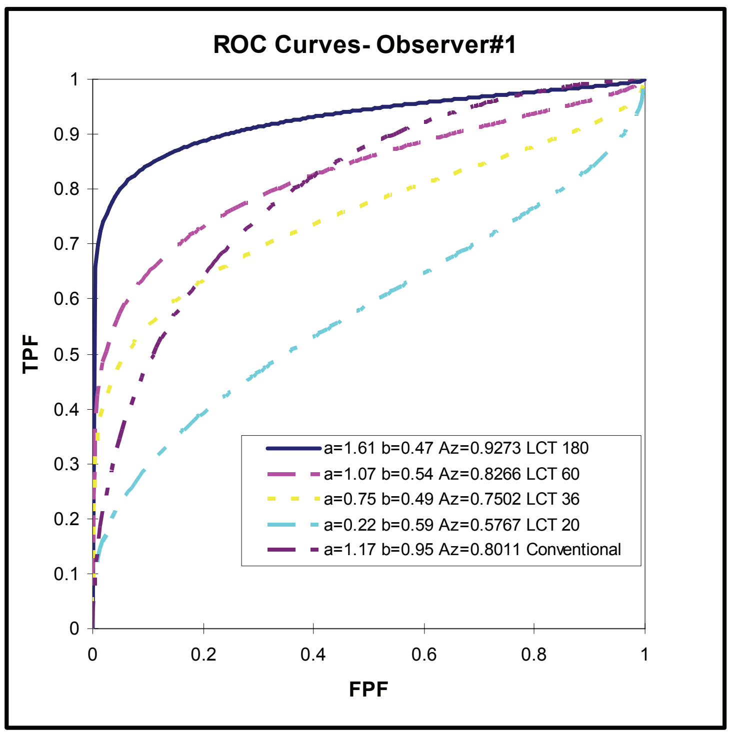

Figure 29. ROC curves for Observer #1.

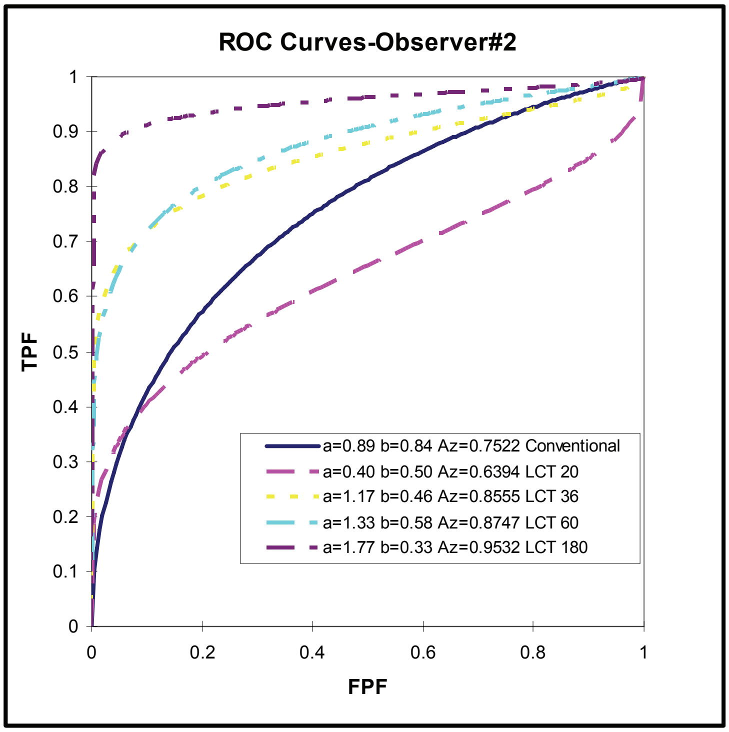

Figure 30: ROC curves for Observer #2.

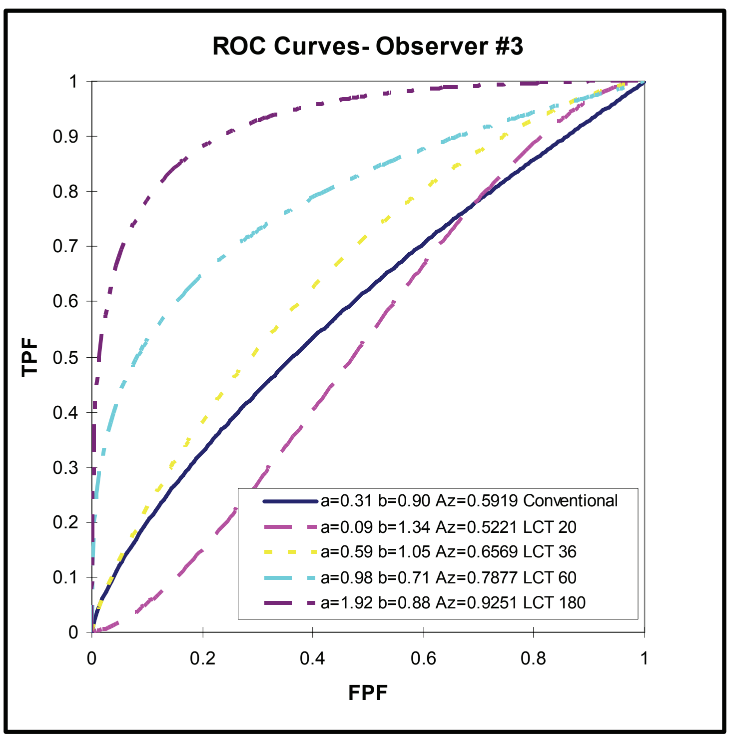

Figure 31. ROC curves for Observer #3.

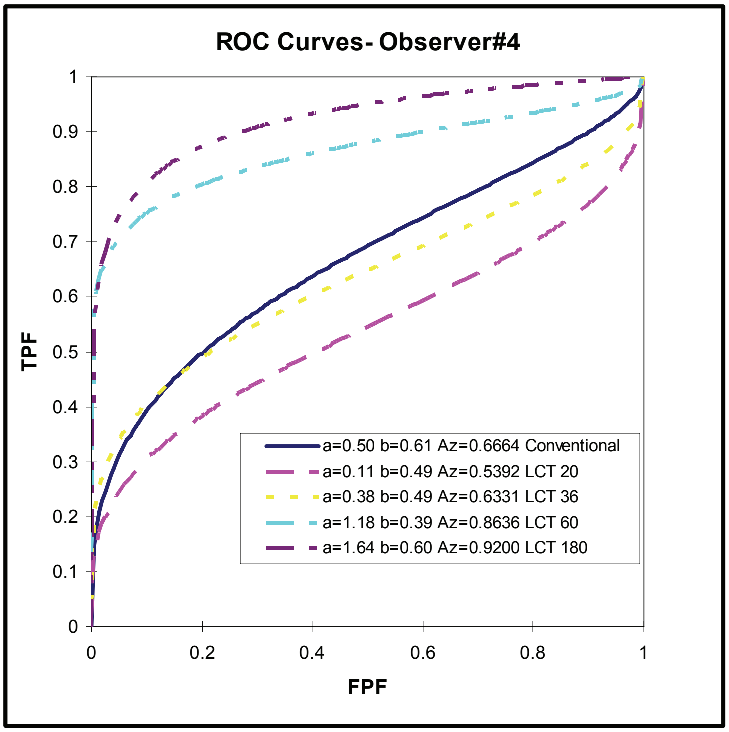

Figure 32. ROC curves for Observer #4.

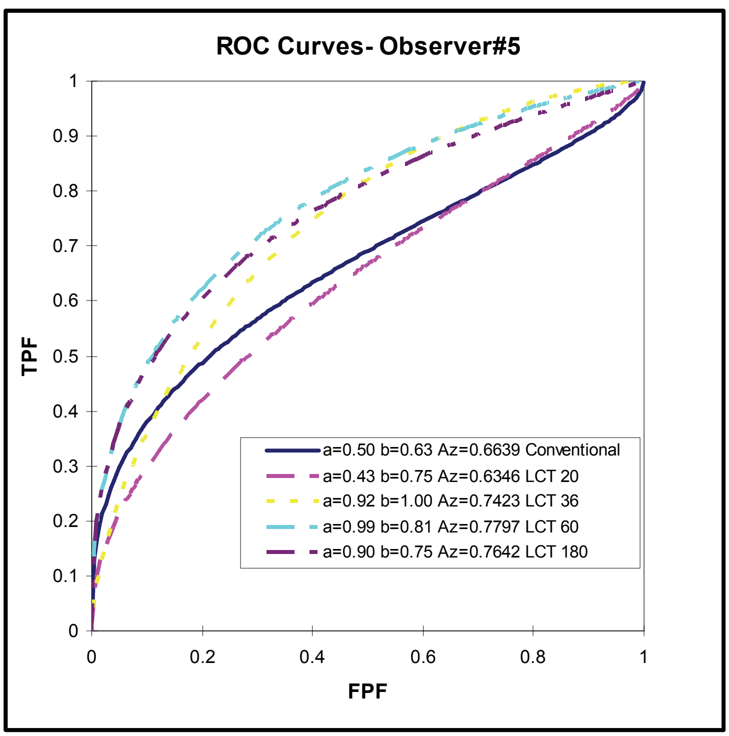

Figure 33. ROC curves for Observer #5.

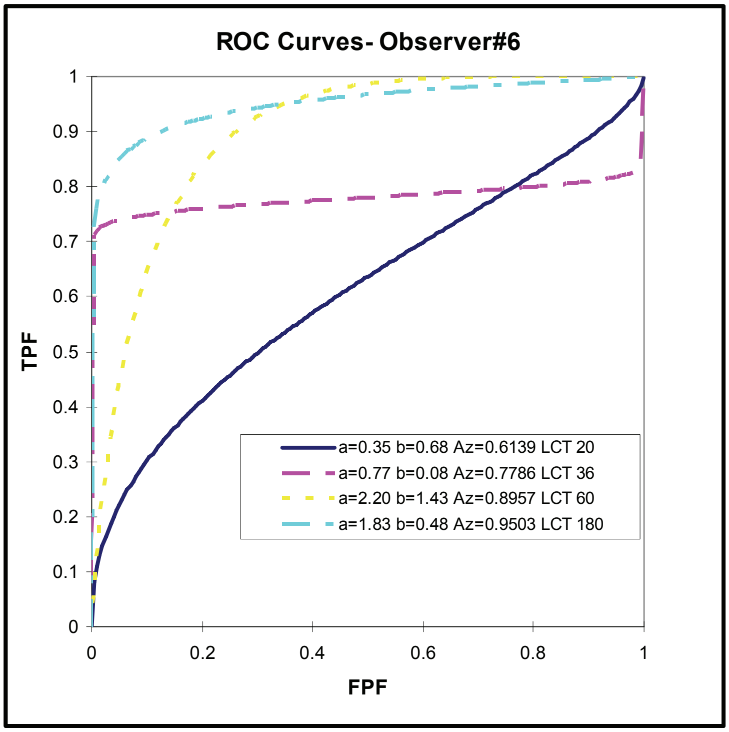

Figure 34. ROC curves for Observer #6.

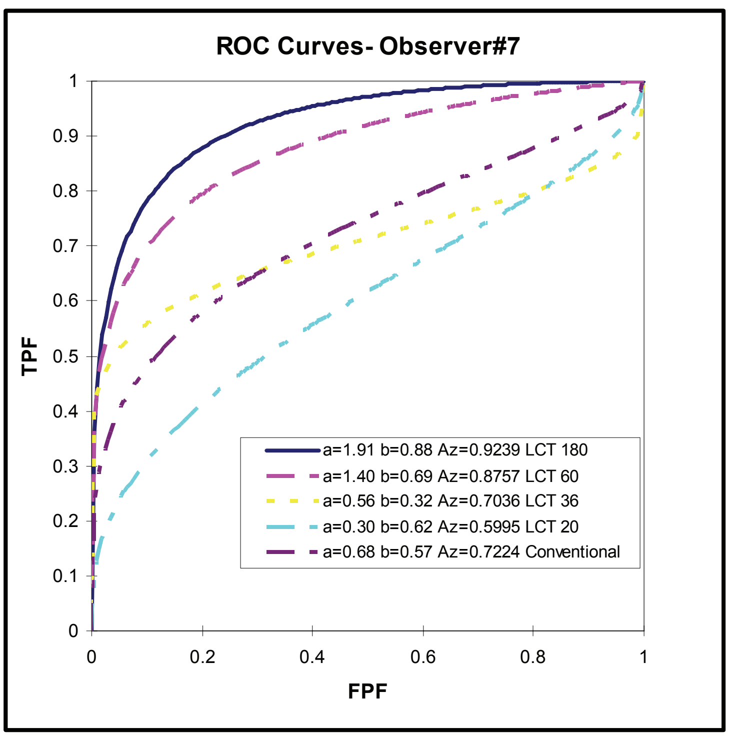

Figure 35. ROC curves for Observer #7.

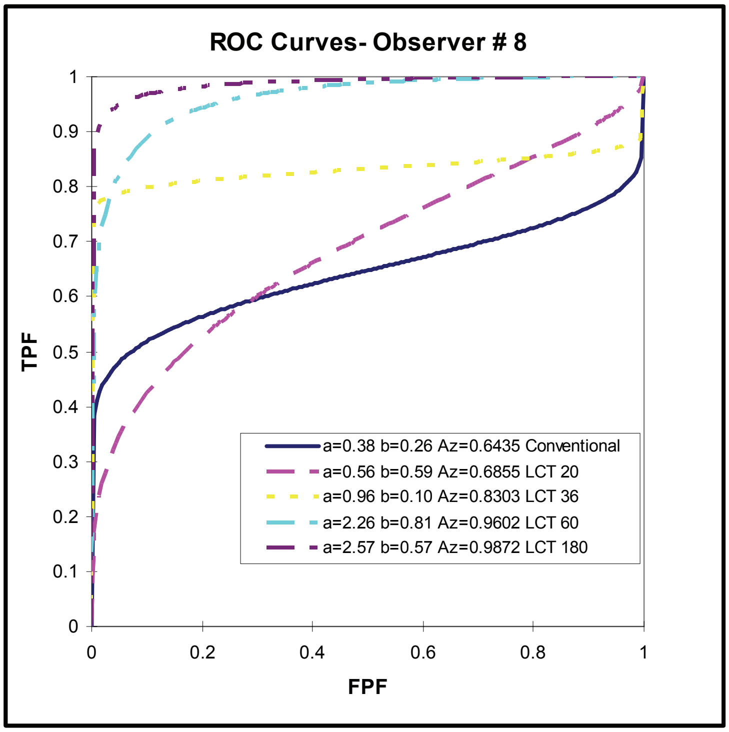

Figure 36. ROC curves for Observer #8.

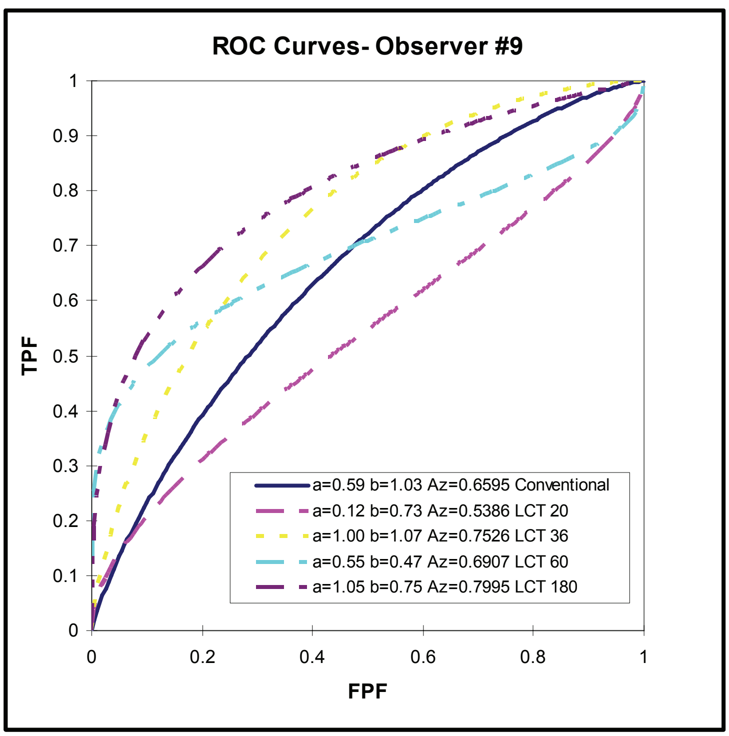

Figure 37. ROC curves for Observer #9.

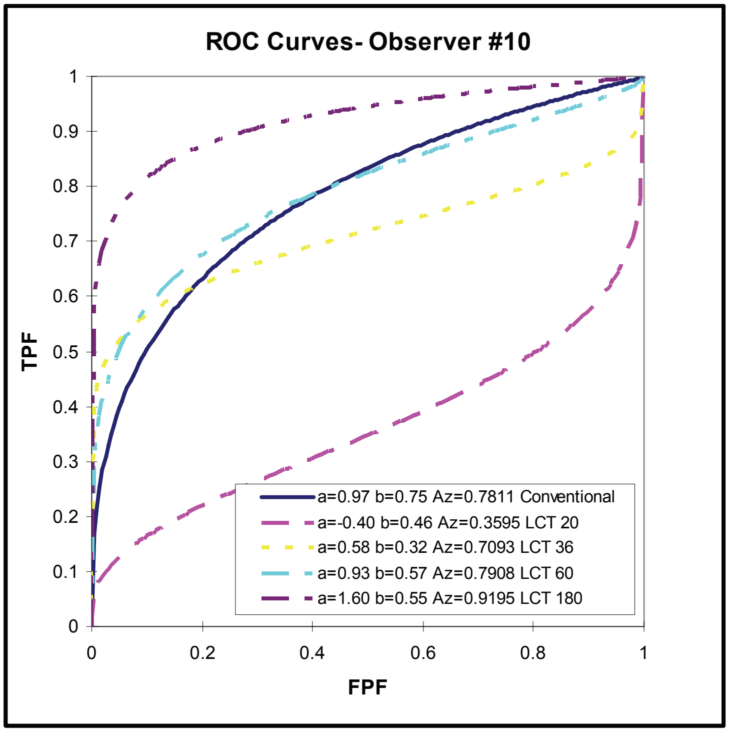

Figure 38. ROC curves for Observer #10.

References

1. Tamse A, Fuss Z, Lustig J, Kaplavi J. An evaluation of endodontically treated vertically fractured teeth. *J Endod* 1999; 25: 506-8.

2. Cohen S, Blanco L, Berman L. Vertical root fractures: clinical and radiographic diagnosis. *J Am Dent Assoc* 2003; 134: 434-41.

3. Rivera EM, Williamson A. Diagnosis and treatment planning: cracked tooth. *Tex Dent J* 2003; 120: 278-83.

4. Walton R. Longitudinal Tooth Fractures. In: (ed). *Principles and Practice of ENDODONTICS.* W.B. Saunders Company, pp 499-519.

5. Holcomb J, Pitts D, Nicholls J. Further investigation of spreader loads required to cause vertical root fracture during lateral condensation. *J Endod* 1987; 277-284.

6. Walton R, Michelich R, Smith N. The histopathogenesis of vertical root fractures. *J Endod* 1984; 10: 48-56.

7. Schetritt A, Steffensen B. Diagnosis and management of vertical root fractures. *J Can Dent Assoc* 1995; 61: 607-13.

8. Walton R. Radiology and endodontics. *Oral surg Oral Med Oral Pathol Oral Radiol Endod* 1995; 80: 495.

9. Hiatt W. Incomplete crown-root fracture in pulpal-periodontal disease. *J Periodontol* 1973; 44: 369.

10. Cameron CE. The cracked tooth syndrome: additional findings. *J Am Dent Assoc* 1976; 93: 971-5.

11. Eakle WS, Maxwell EH, Braly BV. Fractures of posterior teeth in adults. *J Am Dent Assoc* 1986; 112: 215-8.

12. Abou-Rass M. Crack lines: the precursors of tooth fractures - their diagnosis and treatment. *Quintessence Int* 1983; 14: 437-47.

13. Obermayr G, Walton RE, Leary JM, Krell KV. Vertical root fracture and relative deformation during obturation and post cementation. *J Prosthet Dent* 1991; 66: 181-7.

14. Chan CP, Lin CP, Tseng SC, Jeng JH. Vertical root fracture in endodontically versus nonendodontically treated teeth: a survey of 315 cases in Chinese patients. *Oral Surg Oral Med Oral Pathol Oral Radiol Endod* 1999; 87: 504-7.

15. Ehrmann EH, Tyas MJ. Cracked tooth syndrome: diagnosis, treatment and correlation between symptoms and post-extraction findings. *Aust Dent J* 1990; 35: 105-12.

16. Burke FJ. Tooth fracture in vivo and in vitro. *J Dent* 1992; 20: 131-9.

17. Fuss Z, Lustig J, Tamse A. Prevalence of vertical root fractures in extracted endodontically treated teeth. *Int Endod J* 1999; 32: 283-6.

18. Vire DE. Failure of endodontically treated teeth: classification and evaluation. *J Endod* 1991; 17: 338-42.

19. Hansen EK, Asmussen E. In vivo fractures of endodontically treated posterior teeth restored with enamel-bonded resin. *Endod Dent Traumatol* 1990; 6: 218-25.

20. Morfis AS. Vertical root fractures. *Oral Surg Oral Med Oral Pathol* 1990; 69: 631-5.

21. Torbjorner A, Karlsson S, Odman PA. Survival rate and failure characteristics for two post designs. *J Prosthet Dent* 1995; 73: 439-44.

22. Sjogren U, Hagglund B, Sundqvist G, Wing K. Factors affecting the long-term results of endodontic treatment. *J Endod* 1990; 16: 498-504.

23. Endodontists AAo. Cracking the cracked tooth code. *Endodontics: College for Excellence* 1997;

24. Nair MK, Nair UDP, Grondahl HG, Webber RL, Wallace JA. Detection of artificially induced vertical radicular fractures using tuned aperture computed tomography. *Eur J Oral Sci* 2001; 109: 375-9.

25. Nair MK, Grondahl HG, Webber RL, Nair UP, Wallace JA. Diagnostic accuracy of Tuned Aperture Computed Tomography (TACT) in the diagnosis of radicular fractures in non-restored maxillary anterior teeth--an in vitro study. *Swed Dent J Suppl* 2003; 96: 1-93.

26. Tamse A, Fuss Z, Lustig J, Ganor Y, Kaffe I. Radiographic features of vertically fractured, endodontically treated maxillary premolars. *Oral Surg Oral Med Oral Pathol Oral Radiol Endod* 1999; 88: 348-52.

27. Tamse A, Zilburg I, Halpern J. Vertical root fractures in adjacent maxillary premolars: an endodontic-prosthetic perplexity. *Int Endod J* 1998; 31: 127-32.

28. Meister F, Jr., Lommel TJ, Gerstein H. Diagnosis and possible causes of vertical root fractures. *Oral Surg Oral Med Oral Pathol* 1980; 49: 243-53.

29. Bader JD, Martin JA, Shugars DA. Preliminary estimates of the incidence and consequences of tooth fracture. *J Am Dent Assoc* 1995; 126: 1650-4.

30. Tamse A. Iatrogenic vertical root fractures in endodontically treated teeth. *Endodontics and Dental Traumatology* 1988; 4: 190-6.

31. Wenzel A, Kirkevang LL. High resolution charge-coupled device sensor vs. medium resolution photostimulable phosphor plate digital receptors for detection of root fractures in vitro. *Dent Traumatol* 2005; 21: 32-6.

32. Youssefzadeh S, Gahleitner A, Dorffner R, Bernhart T, Kainberger FM. Dental vertical root fractures: value of CT in detection. *Radiology* 1999; 210: 545-9.

33. Fuss Z, Lustig J, Katz A, Tamse A. An evaluation of endodontically treated vertical root fractured teeth: impact of operative procedures. *J Endod* 2001; 27: 46-8.

34. Moule AJ, Kahler B. Diagnosis and management of teeth with vertical root fractures. *Aust Dent J* 1999; 44: 75-87.

35. Groenhuis RA, Webber RL, Ruttimann UE. Computerized tomosynthesis of dental tissues. *Oral Surg Oral Med Oral Pathol* 1983; 56: 206-214.

36. Ruttimann UE, Qi XL, Webber RL. An optimal synthetic aperture for circular tomosynthesis. *Med Phys* 1989; 16: 398-405.

37. Webber RL, Horton RA, Tyndall DA, Ludlow JB. Tuned-aperture computed tomography (TACT). Theory and application for three-dimensional dento-alveolar imaging. *Dentomaxillofac Radiol* 1997; 26: 53-62.

38. Ekestubbe A, Thilander A, Grondahl K, Grondahl HG. Absorbed doses from computed tomography for dental implant surgery: comparison with conventional tomography. *Dentomaxillofac Radiol* 1993; 22: 13-7.

39. Scaf G, Lurie A, Mosier K, Kantor M, Ramsby G, Freedman M. Dosimetry and cost of imaging osseointegrated implants with film-based and computed tomography. *Oral Surg Oral Med Oral Pathol Oral Radiol Endod* 1997; 83: 41-48.

40. Sukovic P. Cone beam computed tomography in craniofacial imaging. *Orthod Craniofac Res* 2003; 6: 31-36.

41. Ning R, Tang X, Conover D, Yu R. Flat panel detector-based cone beam computed tomography with a circle-plus-two-arcs data acquisition orbit: preliminary phantom study. *Med Phys* 2003; 30: 1694-1705.

42. Jaffray DA, Siewerdsen JH. Cone-beam computed tomography with a flat-panel imager: initial performance characterization. *Med Phys* 2000; 27: 1311-1323.

43. Mozzo P, Procacci C, Tacconi A, Martini P, Andreis A. A new volumetric CT machine for dental imaging based on the cone-beam technique: preliminary results. *Eur Radiol* 1998; 8: 1558-1564.

44. Yamamoto K, Ueno K, Seo K, Shinohara D. Development of dento-maxillofacial cone beam X-ray computed tomography system. *Orthod Craniofacial Res* 2003; 6: 160-162.

45. Nakagawa Y, Kobayashi K, Ishii H, Mishima A, Asada K, Ishibashi K. Preoperative application of limited cone beam computerized tomography as an assessment tool before minor oral surgery. *Int J Oral Maxillofac Surg* 2002; 31: 322-326.

46. van Daatselaar A, Dunn S, Spoelder H, Germans D, Renambot L, Bal H, van der Stelt P. Feasibility of Local CT of dental tissues. *Dentomaxillofac Radiol* 2003; 32: 173-180.

47. van Daatselaar AN, van der Stelt PF, Weenen J. Effect of number of projections on image quality of local CT. *Dentomaxillofac Radiol* 2004; 33: 361-9.

48. Arai Y, Tammisalo E, Iwai K, Hashimoto K, Shinoda K. Development of a compact computed tomographic apparatus for dental use. *Dentomaxillofac Radiol* 1999; 28: 245-248.

49. Hashimoto K, Arai Y, Iwai K, Araki M, Kawashima S, Terakado M. A comparison of a new limited cone beam computed tomography machine for dental use with a multidetector row helical CT machine. *Oral Surgery, Oral Medicine, Oral Pathology, Oral Radiology, and Endodontics* 2003; 95: 371-377.

50. Ito K, Gomi Y, Sato S, Arai Y, Shinoda K. Clinical application of a new compact CT system to assess 3-D images for the preoperative treatment planning of implants in the posterior mandible. A case report. *Clin Oral Implants Res* 2001; 12: 539-542.

51. Terakado M, Hashimoto K, Arai Y, Honda M, Sekiwa T, Sato H. Diagnostic imaging with newly developed ortho cubic super-high resolution computed tomography (Ortho-CT). *Oral Surg Oral Med Oral Pathol Oral Radiol Endod* 2000; 89: 509-518.

52. van Daatselaar A, Tyndall D, van Der Stelt P. Detection of caries with local CT. *Dentomaxillofac Radiol* 2003; 32: 235-241.

53. Nair MK, Nair UP, Grondahl HG, Webber RL. Accuracy of tuned aperture computed tomography in the diagnosis of radicular fractures in non-restored maxillary anterior teeth--an in vitro study. *Dentomaxillofac Radiol* 2002; 31: 299-304.